MASTER THESIS

SALT INTRUSION IN THE GHENT-TERNEUZEN CHANNEL

Assessing Salinity Dynamics with Delft3D FM due to Planned Lock Modifications

Author: B. Noordman

DEPARTMENT OF WATER ENGINEERING AND WATERMANAGEMENT (WEM)

EXAMINATION COMMITTEE

D.C.M Augustijn	University of Twente
J. van der Werf	University of Twente / Deltares
F. Hoefsloot	LievenseCSO
W. van Doornik	LievenseCSO

DOCUMENT NUMBER
FINAL - V.01

DATE: 25/08/2016

UNIVERSITY OF TWENTE.

PREFACE

I would like to express my gratitude to my immediate supervisors at the UT and my supervisors at LievenseCSO because of their contributions in my graduation process. From the University of Twent, Denie Augustine and Jebbe van der Werf have helped me to formulate the main outline of my research and they helped to give it a clear structure. Besides this, from LievenseCSO Frans Hoefsloot, Daniel van Putten and Walter van Doornik were daily at hand and ready to help me with the model setup. I would like to thank these people in particular for their help, motivation and commitment. At the time of my graduation project I worked in the Deventer office of LievenseCSO and I had a really enjoyable time with this close and fun group of people. I also would like to thank a number of people at Deltares, in particular Meinard Thiessen and Erik de Goede, for their help in gaining an understanding of the new software package Delft3D FM and their efforts in solving problems which arose along the way. Finally, I would like to thank my aunt Rita for her help in checking the English grammar in the report. Although, it took quite some time, perseverance and help of experts, the final result is satisfactory.

INDEX

ABSTRACT

Saltwater intrusion is a natural phenomenon which primarily exists because of the spatial density differences and it occurs in the fresh-saline transition zone. The Dutch Terneuzen locks, separating the brackish Scheldt estuary and the Ghent-Terneuzen canal [GTC], is an example where salt water intrusion currently occurs. The freshwater inflow from Flanders and the exchange volumes of the locks are the most important variables that influence the salt intrusion in the GTC. Plans have already been agreed and assessed to replace one of the existing locks with a large sea lock, fitting within the current port layout. An environmental impact assessment [EIA] was carried out with the 1D numerical model to estimate changes in the salinity dynamics, however the salinization process in the GTC has much more of a 3D character in view of a salt wedge migration over the seasons.

For this study, a 3D numerical model was built with the new generation hydro software Delft3D Flexible Mesh [Delft3D FM] in order to assess the impact of the planned lock modification on the salinity dynamics in the GTC. The study focused on density flows and density driven salinity transport, approximating the physical flow and transport processes on a more realistic scale. The downstream model conditions were adopted from the EIA, per lock the estimated average tidal exchange of fresh-saline water was explicitly imposed as lock exchange flows, using 3D sinks and sources. With the necessary scaling of the implicitly imposed fresh-saline lock exchange flows, the Delft3D FM model was successfully calibrated and validated with a limited amount of verification data.

The seasonal impacts of the lock modifications were assessed, by simulating various scenarios with the current lock exchange flows and similar for the new situation, with historical inflow series that led to three representative salt intrusion scenarios in the GTC. Longitudinal salt profiles were plotted to visualize the changes in the salinity dynamics. The results of the analysis show that due to the planned lock modifications, the salt intrusion will affect salinity concentrations over the full length of the channel. In winter, the salinity concentrations over the GTC will approximately be twice as high and remain constant over this period. During the low flow period in summer, salinity concentrations increase at least by a factor of 1.8 following the planned lock modifications. Over the complete annual cycle, the relative increase is estimated to be greater upstream.

For this specific case, the 3D modelling gave clearer insights in the density driven salinity transport in the GTC. However, the general conclusions agree with the results of the 1D model used in the EIA. The dynamic behaviour of salinity in the GTC will most likely change, as a salt wedge draws inland and then the gradual salinization of the entire water column follows quickly, even under highly unfavourable freshwater inflows. It can be concluded that the current water quality standards in the GTC are no longer achievable in the near future. Because of the future increase in the salt intrusion, mitigating measures in the new lock will most likely be the best solution, but inherently the local users must be aware and adapt to a more brackish state of the GTC.

Further research should clarify the effects of other factors for a comprehensive analysis, like influences of climate change and economic developments in the GTC, on the tempo-spatial salinity dynamics in the GTC.

1 INTRODUCTION

1.1 General Background

Understanding hydrodynamic processes along coastal zones, rivers, estuaries, lakes and enclosed basins is one of the many fascinating research fields within water management. For years experts have been trying to manage and adapt the water quality and quantity in water systems. In the fresh-saline transition zone, an intriguing phenomenon referred to as 'saltwater intrusion' occurs, which primarily exists because of the spatial density differences.

In the past, empirical relations and methods were developed to gain a better understanding of the saltwater intrusion phenomenon, primarily for basins with an open sea connection (Shaha & Cho, 2009). However, saltwater intrusion is also common in partially closed basins where the exchange of fresh and saline water is driven by the operation of hydraulic structures (Nguyen, 2008). The Dutch Terneuzen locks separating the brackish Scheldt estuary and the Ghent-Terneuzen canal [GTC] is a current example where salt water intrusion is problematic and it forms the subject of this thesis (FDSC, 2015). Over the years, a clear salt wedge is monitored on the bottom of the GTC, varying in size over time and space, which leads to a gradual salinization across the entire length of the channel. The main factors influencing the salinity in the GTC are the freshwater inflow from Ghent and the fresh-saline exchange via the three Terneuzen locks (Vanderkimpen, Pereira, & Mostaert, 2012). The 31 km long GTC is part of the Flemish canal system that drains water from the hinterlands into the Western Scheldt. The Western Scheldt is the middle and lower part of the macro tidal Scheldt estuary, a well-mixed brackish region characterized by a complex morphology (Van Damme, Struyf, & Maris, 2005). An overview of the system is given in Figure 1-1.

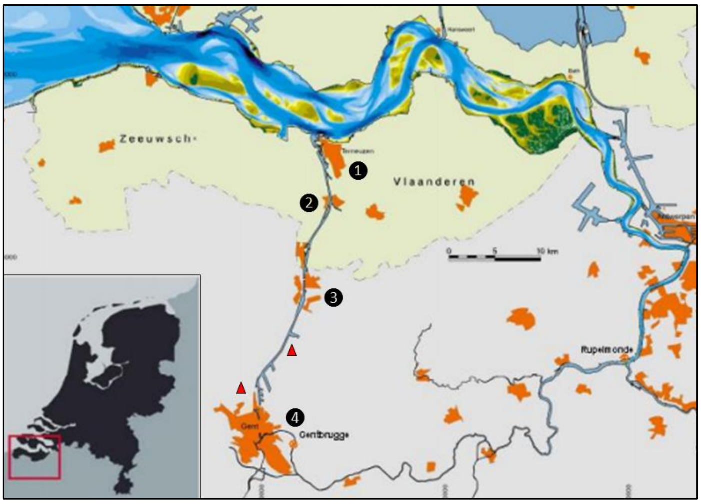

FIGURE 1-1. LOCATION OF THE SCHELDT ESTUARY AND THE GHENT-TERNEUZEN CANAL.
THE MOST IMPORTANT FRESHWATER INLETS ARE MARKED BY THE RED TRIANGLES. CITIES AND VILLAGES ALONG THE GTC ARE MARKED BY ❶ TERNEUZEN ❷ SLUISKIL ❸ SAS VAN GHENT ❹ GHENT.

Future plans to update the Terneuzen lock complex have been made and constructions are planned for 2019. The impact on the salinity dynamics in the GTC has been analysed and evaluated prior to the planned lock modification. However, continuous developments of sophisticated numerical tools allow us to better analyse saltwater intrusion. This thesis will explore this further, using a new tool ''Delft3D Flexible mesh'' [Delft3D FM] which is part of the new generation hydrodynamic software of Deltares (Donchyts et al., 2014).

1.2 Problem Analyses

The Dutch and Flemish Governments signed the mutual cooperation agreement regarding the water systems in the Scheldt estuary basin under the supervision of the Flemish Dutch Scheldt committee [FDSC] in 2005. Analysis of the GTC zone revealed that the maritime accessibility does no longer comply with modern standards, threatening its future operation. A comprehensive research programme was launched to identify alternatives for the nautical Terneuzen port which is situated approximately 500 m inland from the Western Scheldt. Explorative assessments of the transport capacity impact on the locks, including the environmental aspects for the canal zone, were evaluated by the end of 2009. The cost benefit analysis narrowed the search down to three alternatives referred to herein as ''reference designs (Svašek, 2012). Medio 2012, the choice for a large sea lock was made out of the three designs. The implementation of the new sea lock at Terneuzen will change the port lay-out as one of the three locks will be replaced by a much larger lock that allows large vessels of the CEMT-Class Va to have access to the channel (Arcadis, 2007). This will lead to changes in current patterns and salinity dynamics. Consulting company LievenseCSO directed the studies, regarding the environmental impact assessment [EIA], needed for the final selection of the new lock design (FDSC, 2015). Mid 2015, the final EIA was approved by the FDSC.

For years, density driven flows have been a well-known phenomenon in the GTC caused by the exchange of fresh-saline water through locks (Waterloopkundiglaboratorium, 1988); (Callens & Keps-Heyndrickx, 1983). Analyses of periodic depth measurements, performed by the Hydraulic Meteorologic Centre Zeeland [HMCZ], clearly show the presence of isopycnals or density interfaces as a result of saline density flows [APPENDIX III]. These isopycnals, reveal the bi-directional fresh-saline flow in the GTC, which changes in size and direction over the annual seasons.

Managing the salt intrusion in the channel is of major importance, because it forms immediate hazards for agricultural water use and freshwater resources, and threatens the ecological potential of the water system. The secondary effects, like the salinization of fresh groundwater reserves due to brackish seepage, provides even stronger incentives to thoroughly examine changing salinity dynamics as a result of lock modifications (FDSC, 2015). Hydrodynamic modelling was used to analyse the impact of future changes in the salinity dynamics of the GTC. A major issue in the practical conduct of this modelling is the level of detail required to model long-term transport. Given that highly resolved 2DV or 3D simulations can be computationally demanding, generally some compromise is sought in the modelling approach. Within the EIA, long-term salinity changes were estimated using a calibrated hydrodynamic 1D SOBEK model. The magnitude of the fresh-saline exchange of the current locks and the “reference designs” was estimated with a FINEL3D (2DV) model, these results served as boundary conditions in the SOBEK model (Svašek, 2010). As salinization studies in the EIA have already been completed for the planned Terneuzen lock modifications, by Svašek Hydraulics using 1D and 2DV numerical analysing tools, one might question the need for additional research on this subject.

The saltwater intrusion phenomenon is a three dimensional problem and therefore utilizing the new 3D analysing tool Delft3D FM might be more suitable and universal to estimate the salinity dynamics under the various circumstances. The methodology in the EIA applied 1D numerical tools to estimate the depth average transport of salinity in the GTC. This commonly used approach is often believed to be time efficient, computationally effective and adequate to model hydrodynamics under the assumption of well-mixed conditions (Gross et al., 1999). However, the consequence of this method is that density driven salinity transport had implicitly been taken into account by parameterization of salinity transport processes, whilst the dispersion parameter had been enlarged to compensate for the lack of vertical resolution (FDSC, 2015). The recent launch of the new Delft3D FM model gave reasons to assess the present and future hydrodynamic processes in the Ghent-Terneuzen canal, and the resulting depth variable salinity transport processes, with a 3D transport model. Certainly in predicting future scenarios, such as the planned modifications in the lock complex, model results are more reliable if all physical processes are simulated at the correct spatial scale. The impact of density driven salinity transport is unknown and the EIA modelling approach may underestimate its importance, especially under high saline circumstances. Moreover, the current salinization issues provides good test case for this new generation hydro software within which it is possible to work with unstructured grids.

1.3 Research Objectives and Questions

In order to give more clarification on the size and scope of the issues discussed, the following research objectives have been posed:

''To assess a 3D Delft3D-FM model of the hydrodynamics and salinity dynamics in the Ghent-Terneuzen channel and to subsequently use this model to assess the impact of the planned new sea lock on the seasonal salinity behaviour.''

Based on the objective the following research questions will be covered:

i. How can we set-up a 3D Delft3D-FM model of the GTC?
ii. How well can this model reproduce salinity levels in the GTC?
iii. How are the salinity dynamics in the GTC affected by the planned lock modifications?

Due to the absence of measurements of other hydrodynamic variables such as flow velocities, the model can only be compared to salinity data. The hydrodynamics form the basis for the transport of scalar quantities, like salinity. Therefore, all possibilities are examined to accurately reproduce the flow processes and flow patterns in the GTC, but an actual verification with hydrodynamic variables cannot be performed.

1.4 Methodology

This thesis presents a new approach in salinity transport modelling in the GTC compared to conventional 1D methods. The emphasis is on density driven salinity transport that will likely become more relevant due to the planned lock modifications. The model calibration and validation will be performed at various depths (bottom and surface level) instead of the commonly used depth-average approach. By applying scenario analyses, the immediate impacts of lock modifications are reviewed. The advantages and disadvantages of the modelling method will be thoroughly discussed in order to provide a transparent view of the current capabilities of the new generation hydro software.

The methodology in schematizing the GTC system is different from the approach used in the studies for the EIA, but the conditions on the model boundaries are derived from these studies. The results of a detailed model of the locks, developed by Svašek Hydraulics is the best available estimation of the exchange flows and therefore used to derive proper boundary conditions. A full scale physical representation of the locks is beyond the scope and timeframe of this research, thus the same explicit method in the EIA is used to simulate the lock exchange over the downstream model boundaries. The essence of the exchange processes remains the same as with a full physically representation, but simplifications are made to control salt fluxes over the downstream model boundaries.

1.5 Report Outline

A description of the study area is given in Chapter 2. In Chapter 3 a thorough analysis of the historic flow and salinity conditions in the GTC is given, these conditions will be imposed on the Delft3D FM model boundaries. The estimated fresh-saline lock exchange values are adopted from the EIA, but qualitative description is provided on how these exchange flows are estimated. The fourth chapter presents the model setup. Chapters 2-4 will provide answers to the first research question (i). In Chapter 5 the models sensitivity to parameter changes is examined. By visualisation and statistical comparisons the model is then calibrated and validated. The optimized parameter setting is derived to verify the models performance to reproduce salinity levels in the GTC. It answers the second research question (ii). A scenario analysis is performed in Chapter 6 to examine how lock modifications affect salinity dynamics in the GTC. Chapter 7 contains a general discussion wherein the applicability of Delft3DFM for 3D salinity modelling is evaluated. Moreover, it is discussed the uncertainties in the modelling approach. Chapters 6 and 7 answer the last research question (iii). Finally, the conclusions and recommendations for further research are given in Chapter 8.

2 STUDY AREA DESCRIPTION

This chapter provides additional area information, a system analysis of the Terneuzen lock system. Specification of the present locks and the design of the new lock complex is described in detail .

2.1 The Ghent Terneuzen channel within the Scheldt Basin.

The GTC is part of the Flemish canal system and drains water from the hinterlands into the Scheldt estuary. Water from the North Sea naturally intrudes upstream into the freshwater regions of the Scheldt river. The tidal movement, wind and water inlets are affecting the mixing process and thus the salinity distribution along the course of the estuary. The salinity dynamics of the estuary are linked to the salt intrusion of the GTC as it forms the salinity source. Therefore, the variability of salinity in the Western Scheldt, over time, inherently will influence the magnitude of salt intrusion. On average, the tidal range in the outer ports of the lock complex is about 4 m, as water levels fluctuate between the lowest average of - 2.00 m + New Amsterdam water level (NAP), and highest of + 2.00 m above NAP.

The sea channel stretches approximately 31 km, of which 13.7 km is located on Dutch soil and 17.3 km is in Flanders (FDSC, 2015). Along its course, several ports facilitate commercial navigation towards the industrial companies located along the banks. The main channel features the typical characteristics of constructed waterways. In general, the cross-sectional profile is of a rectangular shape. On average, the depth is 13.5 m and the width varies from 120-200 m in the Netherlands up to 350 m in Flanders. For a channel system is the GTC relatively wide and deep. In the near region, only the North Sea canal, situated between Amsterdam to Ijmuiden, is similar in size and even a few meters deeper (Steenkamp et al., 2004; Lebbe, 2009). Near Ghent, fresh water from the river Leie is diverted via the Ringvaart till the weir at Evergem which discharges water into the GTC. The maximum capacity reaches up to 170 m^3/s (daily average), which makes this weir the main supplier of freshwater. Via the Moervaart, Averijevaart, the Tolhuis weir and the Kale, additional discharge is supplied (Callens & Keps-Heyndrickx, 1983). The latter three are not taken into account in this research due to their negligible contributions.

Since the canal construction in 1958, management of water in the GTC is governed by the treaty set up between the Dutch and Flemish governments. The treaty defines the minimal actions from governments to comply with the water policy in the GTC. The water level in the channel is kept constant at around 2.13 m + NAP. The tidal cycles of the Western Scheldt takes an average of 12 hours and 25 minutes, the water level in the channel is during the greater period of about 18 hours per day higher. This favourable situation makes it possible to provide some counter pressure in the salt intrusion in the GTC. Discharging water by gravity is not possible for only a few hours per day.

To ensure that the agreed water level target is controllable and the operability of the lock complex is guaranteed, the Flemish authorities must ensure that the minimum amount of freshwater supply from Flanders is 13 m^3/s averaged over a three summer month period (FDSC, 2015). These summer months are generally May, April and June and mark the low flow period. Currently, the GTC waterway is classified as brackish (0.5 <ppt<30) with low ecological potential and therefore salinization is already partially accepted (Vanderkimpen et al., 2012). The European Framework Directive for water policy has established a salinity target of 3000 mg/l (5.8 ppt), near the Dutch-Flemish border, approximately 1 m below the surface (FDSC, 2015). These target values are classified into specific groups, wherein a good ecological potential value (GEP) should not be exceeded. The minimum flow of freshwater from the Ghent canal system is set to provide adequate counterbalance to the salt intrusion. This minimal flow limit however, is presently already difficult to achieve in the dry summer months. The data analyses carried out in Section 3.2 elaborates further on the observed flow conditions and historic salinity levels in the GTC and the Western Scheldt.

2.2 The Terneuzen Lock Complex

The Terneuzen lock complex consists of three locks operating on a number of guidelines. RWS Zeeland has defined its functions in the Management and Development Plan of National Waters [MDPNW] (in order of priority):

- Flood protection and drainage of the GTC
- Traffic management
- Mitigating measures for salt intrusion

2.2.1 Flood protection and drainage of the GTC

The present lock complex consists of three locks and are denoted by their geographical location respectively: the Western, Middle and East lock (Figure 2-1). The Western lock is the largest and enables large size vessels of the category (CEMT III-IV) access to the channel. The Middle lock is mainly used for passage of medium-sized barges (CEMT class I-II). The Eastern lock is used for recreational shipping (CEMT Class 0). The main lock specifications are displayed in Table 1.

FIGURE 2-1. THE TERNEUZEN LOCK COMPLEX, VIEW IN NORTHERN DIRECTION (SOURCE: ARCADIS, 2007)
FROM LEFT TO RIGHT: THE WESTERN, MIDDLE AND EASTERN LOCKS.

TABLE 1. LOCK SPECIFICATIONS (VANDERKIMPEN ET AL., 2012).

Lock	Dimensions			Max. Q
	(L x W x D)	Bottom	Sill Height	Daily Averaged
	[m]	[m + NAP]	[m + NAP]	[m³/s]
Eastern	270 x 24 x 4.5	-6,50	-4,50	90
Middle	140 x 18 x 8.6	-7,58	-6,22	85
Western	290 x 40 x 13.5	-13,44	-11,44	130

The locks are controlled to fulfil the requirements defined in the MDPNW as good as possible under varying hydrodynamic conditions, in both the Western Scheldt and the GTC. The locks are designed to provide protection, by peak discharges or extreme water levels in the estuary, preventing the landscape behind it from flooding. Within the lock complex there is no separate sluice that controls the GTC level and water is drained into the Western Scheldt via the locks. This occasionally affects the operability of the locks with respect to navigation. When the water level in the GTC is higher or equal to the level in the Western Scheldt, water cannot be discharged from the channel. Shipping is then temporarily halted in all locks, since freshwater from the canal is used to level the lock cambers. Under average tidal conditions in the Western Scheldt, the water level difference allows to discharge water from the GTC into the outer ports by gravity. As Table 1 shows, on a daily average basis, the maximum total discharge can be raised to 305 m^3/s in extreme discharge events. At times when great amounts of water must be drained from the Flemish canal system via GTC, shipping will be gradually halted for each lock consecutively based on the rise in water level. Regular coordination is required between the upstream inflow at and the outflow via the Terneuzen locks to prevent large water level fluctuations. First, water is discharged via the lock culverts in the Middle Lock and optionally by partial opening of the lock doors. Discharging via the Middle Lock begins as soon as the target level of 2.13 m + NAP is exceeded and reaches a maximum at a level of 2.23 m + NAP. When this appears insufficient, the Eastern Lock is subsequently used. Discharging through the levelling valves in the Eastern Lock begins at a level of 2.23 m + NAP and reaches a maximum at 2.33 m + NAP. The Western lock is only used as a last resort in floods. The draining for flood alleviation through lock culverts in the Western Lock begins at a level 2.33 m + NAP and reaches a maximum at 2.43 m + NAP. If a lock is used for flood management, navigation is no longer possible through the respective lock.

2.2.2 Traffic management

Shipping happens in both directions, as the GTC water level is higher for the greater part of the day compared to the level of the Western Scheldt, so the lock chambers needs to be levelled. The water level in the lock chamber is levelled to the channel level, at each lock cycle with fresh or low brackish channel water. The course of this process is discussed in more detail in section 3.2.3 and visualised in Appendix I. Lock cycles A large part of the relative fresh channel water is lost due to the levelling of the locks, which means the remainder of available water or the flow rate through the locks, is very limited in summer. When the inflow of water from Flanders is sufficient to level the locks, the water level in the GTC is kept practically constant by discharging small amounts of water through the Middle and Western locks. The Western and Middle locks are equipped with fill-and emptying systems. Lock culverts are installed in the locks which are both used to level the locks chambers and to discharge excess water in-between locks operations. This eliminates the need for a separate sluice in the present complex.

2.2.3 Mitigating measures for salt intrusion

To hamper the saltwater influx via all locks, air bubble screens or air curtains are installed at both the northern and southern lock sides. In principle, air screens create barriers that partially block the density currents, occurring immediately after opening of the gates. Still, the effect of this measure is limited and affected by many other factors. Within this thesis no further research into all these salt reducing factors is carried out. However, in the determination of the fresh-saline exchange of the locks this is explicitly incorporated.

Additionally, the unique fill-and emptying system in the Western lock acts as a measure to mitigate the influx of saltwater. As water is discharged via the locks culverts to control the target water level, the saline density flows caused by lock operations in direction of the GTC, can directly or indirectly be flushed back to the outer port by gravity. Apart from the mixing of fresh and saline water, the largest part of the saltwater flux will be captured by a local bottom drop in front of the Western lock. This salt trap functions as a temporarily storage of saltwater as heavier saline water descends to the bottom. Nowadays, the extraction of salt water from the salt trap occurs in between the lock operations and not during, as it was originally conceived (Lebbe, 2009). The salt trap is too small in size and therefore it spills saline water in some instances, because of the large number of lock operations. Moreover, the salt trap is silted, making it less effective over the time. This explains why throughout the year a salt wedge is visible on the bottom in proximity of the locks. On its own, the salt trap has no effect on the saltwater influx but in conjunction with the discharging through the lock culverts, an effective method is created to flush high saline water back into the outer ports.

In order to mitigate salt intrusion through locks, many systems have been developed that prevent the primary exchange of salt water. The principle of the Terneuzen system is however based on the reduction of the incoming salt flux after it has ended up in the channel. Therefore, density flows into the GTC occur to a large extent, causing the relatively saline content of the lock chamber to exchange with the channel. Subsequently the saline influx is flushed back with the lock outflows. Part of the incoming saltwater flux mixes with the relatively fresh channel water which means there is effectively more fresh water required to mitigate salt intrusion. Substantial amounts of fresh water are required for this and during low inflow periods from Flanders it is known that the fresh water quantity is less than the product of the incoming saltwater fluxes as a result of lock operations. This forms the roots of the annual salinization problem.

2.3 Planned Lock Modifications

The new sea lock will be integrated into the existing lock complex, a new lock will replace the Middle lock. The new lock will be longer, wider and deeper than all existing locks and slightly changes the Terneuzen port layout (Figure 2-2). The new sea lock will become 427 m in length, 55 m wide and 16 m deep (FDSC, 2015). Thereby, ships of category CEMT IV and Va, the largest classes of inland shipping, can enter the GTC (Arcadis, 2007). The new design is similar to that of the Western lock but without the installation of mitigating or reducing measures. It is therefore a given fact that to some extend an increase in salt intrusion has been accepted in the choice of this new lock complex. The potential amount of saltwater in the new lock chamber is far greater. Based on the dimensions, the estimated salt flux accompanied by lock exchange flows is 2.3 times greater in the future scenario (Svašek, 2010). No information is available about the required quantities of freshwater to level the new lock, but the discharge rate will increase equally. The land tongue between the existing Middle and Western lock, visible in Figure 2-1, will also be removed and a separate drainage facility will be constructed east of the Eastern lock. This means shipping no longer needs to be obstructed by the locks at times of discharge peaks in the GTC.

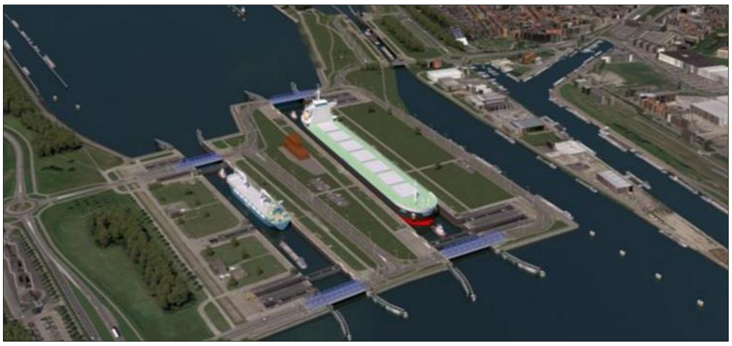

FIGURE 2-2. DESIGN OF THE MODIFIED LOCK COMPLEX. SOURCE: (FDSC, 2015)

3 HYDRODYNAMICS & SALINITY IN THE GTC

The reliability of data is important for numerical flow modelling. Flow equations are well known and the Delft3D FM software has already proven to be able to calculate hydrodynamics and salinity dynamics accurately for various different purposes, primarily in macro scale basins (Santosa et al., 2014 ; van Drakestein, 2014). Still, the reliability of model output depends mainly on the efforts of the modeller, the accuracy of the input data and the data used for calibration and validation.
To understand the general dynamics in the GTC, and to determine inconsistencies and/or uncertainties in discharge and salinity data, a thorough data analysis is performed.

3.1 Data Sources

The data for this study is gathered from the data sources listed in Table 2. The table distinguishes between the Dutch and Flemish databases. The LMW (Dutch) is a collective name of several existing Dutch databases that have recently merged into one national register of water-related data, including the database Dutch data storage of national waters (Dutch: DONAR) and monitoring network Zeeland Tidal Waters (ZEGE).

TABLE 2. OVERVIEW OF DATA SOURCES.

Database	Source	Domain	Variable	Metric Unit	Frequency
LMW (NL)	HMCZ	Western Scheldt	Chloride level	mg/l	10-Minute
	RWS	Terneuzen Locks	Discharge	m^3/s	Daily
	HMCZ	GTC	Chloride level	mg/l	10-Minute
TSO (NL)	HMCZ	GTC	Salinity	ppt	2-Monthly
WI (BE)	HIC	Ringvaart, Moervaart	Discharge	m^3/s	Daily

As already mentioned in the research objective, estimates of the exchange flows are imposed on the downstream model boundaries. The approach, in deriving the fresh saline exchange at the locks and the resulting exchange volumes and exchange flows, is discussed later in this section after the flow and salinity conditions are determined at the upstream and downstream boundaries.

The listed data sources express salinity as the concentration of chlorides in grams per cubic meter of water. Delft3DFM computes salinity as the total concentration of dissolved salts in total parts of dissolved salts per thousand parts of water [ppt = g/kg]. Because the content of other dissolved salts is much lower than the chloride content and in addition the impact of temperature fluctuations and salt concentrations on the density of water is probably limited to a few percent, this inaccuracy in comparing data sets is neglected in the light of other uncertainties like measurement errors and data inconsistencies. To convert chloride concentrations in g/l to salinity in ppt, the following empirical relationship is used that accounts for the contribution of chloride ions to the total salinity concentration and the density of seawater (UNESCO, 1996):

$$\mathrm{S} = 1{,}80655\ \mathrm{CL}^{-} \qquad \text{EQUATION 1).}$$

In which:

S = salinity [ppt]
Cl^{-} = chloride concentration [g/l]

3.2 Deriving Boundary Conditions

3.2.1 Downstream boundaries

Discharge data through the locks, for a period of 15 years, were obtained from the Dutch national water measurement network LMW. This data contains the daily average outflow per lock, which is calculated by RWS and is the only consistent discharge data available on the outflow of the GTC. These outflows relate to the effective volumes of relatively fresh water that are lost in the levelling process and the daily discharge rates through the lock culverts to control a constant water level.

As stated in section 2.2, the prioritization of the various lock functions and the chronological operation of the locks is defined in the MDPNW. This policy is clearly reflected in the data as discharge rates per lock are very different each day. The Eastern lock is only used when there is a very high water supply and is therefore largely only used for shipping. If the inflow is around the order of magnitude of the minimum flow rate of 13 m^3/s, only then is excess water discharged through the culvert system of the Western lock. If the freshwater inflow is higher, then the middle lock will also be deployed. The levelling losses on the locks are relatively constant over the time series. The average loss on the Eastern lock is 2.56 m^3/s, and the Middle lock 0.48 m^3/s. The loss on the Western lock is on a daily average 3.4 m^3/s, but the time series shows greater variation between days.

By summing all locks outflows, this data gives an indication of the long-term variation of the flow conditions in the GTC. Both the inflow from the canal at Evergem and Moervaart streams determine the flow regime in the GTC. Minor deviations occur between the inflow and outflow of the GTC, which results in small water level fluctuations. To maintain the target level of 2.13 m + NAP with maximum permitted deviations up to 25 cm, the discharge rate of the Terneuzen locks needs to be adjusted to the supply of freshwater from Flanders. In Figure 3-1 the cumulative outflow time series are plotted over the period 2008-2015. The data for the period 2000 to 2008 has been omitted since during this period no accurate salinity data exists in both the Western Scheldt and the canal.

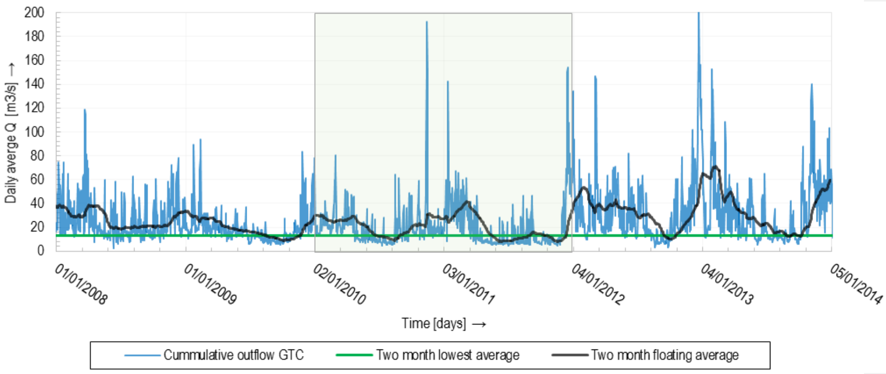

FIGURE 3-1. TOTAL OUTFLOW OF THE THREE LOCKS FROM THE GTC TOWARDS THE WESTERN SCHELDT OVER THE PERIOD 2008-2014.

The total outflow or discharge data is provided on a daily basis and shows great variations between subsequent days. A clear annual periodicity can be observed with seasonal periods of high and low discharge. The years 2010 and 2011 are marked within a light blue box as these two years have a representative flow regime that eventually led to very different salt intrusion scenarios. The latter will become apparent when the measured salinity concentration in the GTC are shown. Overall, the outflow from roughly April to September is fairly limited in comparison to the rest of the year. The floating average trend line in Figure 3-1 reveals that the discharge in the summer months is systematically lower. As defined in the treaty, the lowest average inflow is assessed over a period of two months. Minima in summer can fall back to 8.4 m^3/s averaged over two months, while the international treaty appoints a minimal average supply of 13 m^3/s over the two lowest summer months. Over the whole period, on average 3.5 months do not meet the before mentioned standard discharge (FDSC, 2015). The duration of the water shortage period determines the magnitude order of the salt intrusion for the greater part, it is in this period that a salt wedge starts moving upstream.

As will be substantiated, the shortage of fresh water in summer plays an important role in the intrusion of saltwater. In these periods there simply is not enough water supply to flush out the incoming saltwater fluxes from the system. On the other hand, occasionally high discharge peaks are obtained in summer, the total outflow temporarily rise far above the minimal supply of 13 m^3/s. Most of the discharge peaks between subsequent days are caused by a temporal abundance of water. In the summer months, heavy showers sometimes fall within the Scheldt basin which must be able to be quickly discharged via the Flemish canals. During these events, all locks are used to drain excess water. This has a positive effect on the reduction of the salinity intrusion because in a short period a relatively large amount of salt is flushed back towards the Western Scheldt. A part of the temporary discharge increase in the summer period is as a result of the policy regarding salt reduction. If salinity levels rise too quickly, than through dialogue between RWS and the Flemish governing authorities, more water can temporarily be supplied via the weir of Evergem to create flush regimes. The winter discharge also shows a significant variance in over the time series 2000-2015. By estimating the seasonal average discharge, respectively the period from mid-autumn to mid-spring, it elucidates the long-term average flow conditions. On long-term average the winter flowrate is 31.4 m^3/s and the summer flowrate is only 16.6 m^3/s.

The salinity of the lock outflows are fully dependent on the time variable conditions in the GTC and this will be reproduced with the Delft3D FM model. The salt fluxes that enter the system daily, as a result of the exchange flows, are dependent on the tidal dynamics of the Western Scheldt. To derive the salinity constituent of the incoming salt water fluxes, the long-term variation of salinity in the Western is displayed in Figure 3-2. The data comes from the LMC and is measured by the HMCZ over the period 2008-2013.

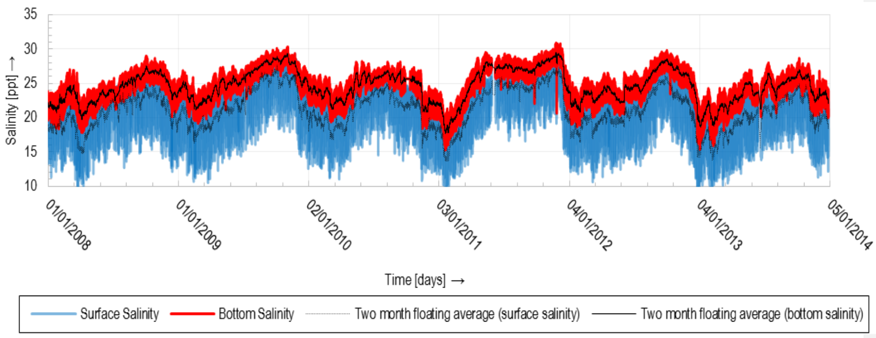

FIGURE 3-2. HISTORIC SALINITY CONCENTRATIONS IN THE OUTER PORT OF THE WESTERN LOCK, IN THE WESTERN SCHELDT.

The measuring station (TWZZ), where the data is measured, is at the south side of the Western lock. The two monthly floating average trend lines are added in black, in order to highlight the general behaviour of salinity. The surface salinity shows more fluctuations than the bottom salinity. In the outer port of the Western lock, surface and near-bottom salinity is measured at a vertical reference level of -2.5 m and -10.0 m +NAP. The data in Figure 3-2 show a dynamic equilibrium in the salinity values over the years, similar to the annual periodicity in the total lock outflow in Figure 3-1. It appears that there is a clear correlation between the salinity and the outflow to the Western Scheldt (Vanderkimpen et al., 2012). Halfway through the spring the flow decreases because of a natural depression in the Scheldt water supply, as results the average salinity concentrations over the tide increase. The vertical salinity gradients in the Western lock indicate some degree of stratification. The difference between the two salinity records in Figure 3-2, measured at different water depths is maximal 7.4 ppt and on average 3.2 ppt.

3.2.2 Upstream boundaries

To derive the upstream model conditions and to impose these on the Delft3DFM model, flow and salinity data has been collected from the inflow streams, the Ringvaart and Moervaart. Only since the beginning of 2011, daily discharge measurements are available from Hydraulic Information Centre (HIC) for both inflows, however this data is inconsistent and has value gaps.
The measurement frequency is equal to that of the outflows. It can be assumed that the cumulative discharge of the two visualized data sets is of approximately the same order magnitude as the cumulative outflow through the lock complex. After all, the storage capacity of the GTC is approximately 10^6 m^2 times 0.25 m. During discharge peaks over 100 m^3/s, the storage capacity is reached after only 7 hours. Therefore, the outflow has to respond quickly and equal the inflow to maintain the target water level. In exactly the opposite way, this perspective is also true as during periodic low inflow, the outflow will be lowered through the locks because it is known that no more fresh water is available. However, it appears that there is a not negligible difference in the cumulative inflow and outflow, therefore both upstream data sets cannot be used. During low inflow periods in the summer, the daily average is only about 2 m^3/s, but in winter the difference is sometimes more than 5 m^3/s. By assuming that the outflow of the GTC is strongly correlated to the cumulative inflow of the system, the inflow will be derived from the data in Figure 3-1.

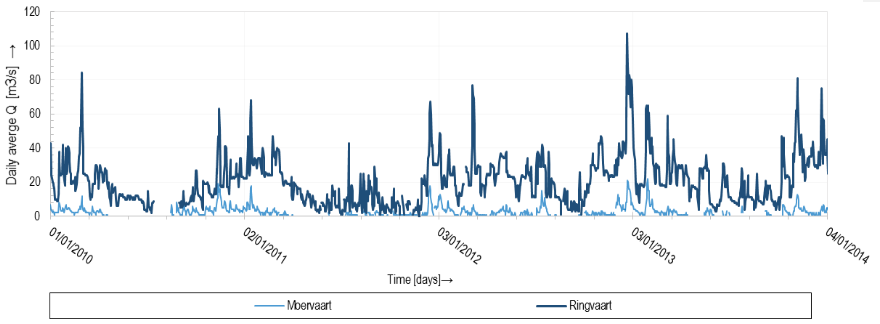

FIGURE 3-3. UPSTREAM INFLOW INTO THE GTC OVER THE PERIOD 2010-2014.

The decision is made to use the outflow data, not only because it is considered more reliable and more complete, but also because there is information about the outflow between the various locks. Within the model setup, a discharge distribution has to be used to define the source of the inflow. The discharge distribution in Figure 6 shows temporal variation but cannot be adopted due to the inconsistency of the measurements. Therefore, the model setup imposes a constant discharge distribution of 0.88 from the Ringvaart and 0.12 from the Moervaart, this is the average distribution over the entire time series in Figure 3-3.

3.2.3 Estimation of the exchange flows

This section elucidates how the lock exchange flows are quantified and elaborates on the variables in the estimation of the exchange flows. To enable navigation between the GTC and the Western Scheldt, the locks are used for lifting and lowering of vessels. Traffic occurs in two directions, upstream towards Ghent or downstream in direction of the Western Scheldt. The vessels enter the lock chamber and the water level in the chamber is levelled towards the desired direction. The movements of both opening and closing of the lock gate is denoted as a full lock cycle. A cycle has multiple phases that influence the salt load in the lock chamber to be exchanged with either the canal or the outer ports in the Western Scheldt. To illustrate the flow processes in the lock chamber directly after opening of the inner or outer doors, Appendix I shows a schematic representation of the Western lock (Deltares, 2012).

After the levelling process is completed, the lock gates open and an exchange flow will occur with the highest density moving over the lock bottom and a lower density current moving near the free surface in reverse direction. The greater the density differences, the faster this exchange process will occur. The main indicator showing how much water is exchanged is the gate opening time. The lock exchange water volume increases the longer it takes for vessels to enter or leave the locks. However, the full lock volume will never be completely exchanged due to the geometry of the locks. Lock sills, partitioned near the lock heads, form barriers that partially block the horizontal movement of saline density flows over the lock bottom. The navigational direction of vessels determines where the lock volume is exchanged. Only at the opening of the inner lock door will there be a salt influx in the channel. The emphasis in this paragraph therefore lies on lock operations following vessels that enter the GTC and refers to the third phase, described in Appendix I. Lock cycles.

The method used, to estimate the volume of the exchange flows, is through examining the decrease of the initial salt load in the locks as a function of the opening time of the inner lock door. The initial mass of salinity, or the total salt load in the lock chambers depends on the preceding exchanged lock volume, the lock geometry and the velocity of the exchange process. The maximum saltwater volume to be exchanged is never fully reached, a mixed layer will remain behind the lock sills. The maximum exchange is reached when the gate opening time becomes larger than the time for the brackish water, to be reflected by the outer lock gate. The low saline water forces the remaining saltwater above the lock sill out of the lock chamber as the internal wave circulates through the lock (Appendix I step 3). An equilibrium is reached when there are no more exchange flows between the lock chamber and the canal. The same process occurs for lock operations in the opposite direction, although instead of exchanging the lock chamber with brackish canal water, the water in the lock chamber is replaced with saltwater from the outer ports.

To derive the downstream boundary conditions for the Delft3DFM model, the results of Svašek Hydraulics (2010) were adopted. By a series of detailed numerical 2DV simulations using a FINEL3D model, the exchange volumes were estimated for the existing Terneuzen lock complex, as well as for the new sea lock scenario. The exchange volumes are then converted into lock exchange flows by distributing total exchange volumes based on the number of lock operations over a single day. The approach, for all locks, takes into account a reduced salt flux as a consequence of the activation of the air screens on both lock heads. Additionally, for the Western lock, indirect back flushing of salt water from the saltwater trap is included in the calculation.

shows the resulting salt load in the chambers as a function of time for all locks. In nearly all scenarios, the initial decline of salinity in the lock chamber is practically linear and in proportion to the total salt load inside the chamber. Likewise, the total salt load is linear dependent on the water levels in the outer ports (Svašek, 2010). As water levels in the outer port fluctuate through tidal movement, baseline simulations were done respectively for the average tidal conditions in the outer ports, the average tidal sea level [MSL], the mean of the highest tidal sea level [MHL] and the mean lowest tidal average level [MLL].

After opening the inner door for a certain time, the exchange process slows down and stops as the density difference between the GTC and the lock chamber disappears. If the time required navigating vessels in the lock chamber is longer than the exchange time, it is known that, depending on the lock geometry, the exchange volume is at a maximum. The FINEL3D model simulated time to fully exchange the lock content [TLE] is therefore compared with the average door opening time that, in turn, is determined by a SVIVAK model. The mean opening times were estimated using SIVAK, this is a forecasting tool that gives a highly detailed simulation of the movement of vessels through a network of waterways and hydraulic structures. This way, the average passing time and lock occupations were determined for varying shipping scenarios and different lock configurations. The SIVAK model included empirical data based on the Dutch inland waterways and inland waterway fleet (Lamboo, 2014). The TLE at MSL, the average door opening time [ADT] and ratios are summarized in Table 3.

TABLE 3. ESTIMATES OF THE EXCHANGE TIME (SVAŠEK, 2010).

Lock	TLE (min)	AGT (min)	Ratio ADT / TLE
Eastern	8	30	3
Middle	16	30	2
Western	13	45	3
New	20	60	3

The ratios denote that the exchange process for all locks had been completed thus the full lock content will be exchanged, however this does not necessarily mean that the total salt load was exchanged. A substantial part remained in the mixed layer behind the lock sills and will not be exchanged. On average, the density difference between the inner lock doors and the GTC was assumed to be 25 kg/m^3 in the final simulations of the lock exchange rate and volume (Table 4). The results from FINEL3D simulation demonstrate that the exchange ratio of the Eastern lock is significantly lower than the other locks. The horizontal momentum created by the density flows in the Middle, Western and the new lock enables the salt wedges to partially jump over the locks sills. (Svašek, 2010). The saltwater and simultaneously the brackish water fluxes, imposed explicitly as exchange flows with a salinity constituent, are the translation of the simulated lock exchange volume time and the average number of lock cycles computed with the SIVAK simulations distributed over one day. The salinity constituent is composed from the average salinity in the Western Scheldt, displayed inFigure 3-2. The exchange flows per lock are displayed in Table 5.

TABLE 4. ESTIMATION OF THE EXCHANGE VOLUME PER LOCK WITH FINEL3D OVER THE ADT (SVAŠEK,2010).

ID	Width	Length	Bottom	MSL	Ratio Exchanged volume/Total lock volume	Exchange
(Lock)	(m)	(m)	(m+NAP)	(m+NAP)	FINEL3D [-]	Volume (m^3)
Eastern	24	260	- 7.0	0.08	**0.30**	4.0×10^3
Middle	24.5	140	- 7.5	0.08	**0.81**	1.7×10^4
Western	40	290	- 12.82	0.08	**0.93**	1.3×10^5
New	58	462	- 17.0	0.08	**0.68**	2.1×10^5

The temporal distribution implies a constant saltwater flux and a freshwater flux as the return flow towards the outer ports spreads evenly over the day. The exchange process is highly dynamical in time and the exchange flows are marked by their pulsating behaviour rather than a constant flux in-out of the domain. However, initially for the model setup in Delft3DFM, the exchange flows in the present situation are adopted from FDSC (2015).

TABLE 5. ESTIMATION OF THE DAILY CONSTANT EXCHANGE FLOWS (SVAŠEK, 2010).

Lock	Present Situation		New Situation	
	Daily Nr. Operations SIVAK	Exchange Flows (m^3/s)	Daily Nr Operations SIVAK	Exchange flows (m^3/s)
Eastern	18.95	0.88	18.95	0.88
Middle	9.73	1.93	-	-
Western	13.84	20.73	13.84	20.73
New	-	-	10.37	25.39

Within the calibration procedure it is determined whether the magnitude order and temporal constant distribution of the salt fluxes results in representative salinity levels in the channel. If the mitigating function of the Western lock cannot be properly integrated in the Delft3DFM model, than it is necessary to lower the exchange flows. The salt fluxes on the downstream boundaries must be in balance, otherwise artificial high salinity levels will occur. This explains why the water inflow is sometimes even lower than the total incoming saltwater flux in Table 5. Logically, the vast majority of the exchange volume of the Western and the New lock will be flushed back with the lock outflow.

3.3 Verification Data

On the Dutch part of the channel, salinity is measured at three static stations with a 10-minute frequency (Figure 3-4). It provides a good perspective of the tempo-spatial salinity distribution in the GTC. Similar to the discharge regime in the GTC, an annual dynamic equilibrium is seen in the salinity levels. Vanderkimpen et al., (2012) and Steenkamp (2004), concluded already that the upstream discharge has the largest influence on the salinity in the channels. The trend of the measured salinity lines indeed shows a high correlation with the trend line in Figure 4. Overall, the time series show no increasing trend in the salinity levels, but with some regularity the salinity levels exceed the EWFD water quality standards. Vertically, each station measures salinity at two points that are referred to as the “surface and bottom” salinity. This salinity data is gathered from the LMC database and is fairly consistent and complete for all observation stations for the period of end 2007 to 2011. The salinity data for the Dutch part of the GTC is shown in Figure 3-4 and over lapses with the lock outflow data. The TWKZ station lies only 500 meters from the locks, the KGTB station is situated at the bridge of Sluiskil circa 3.5 km upstream and the KGTS station lies 10 km upstream near the Belgium border.

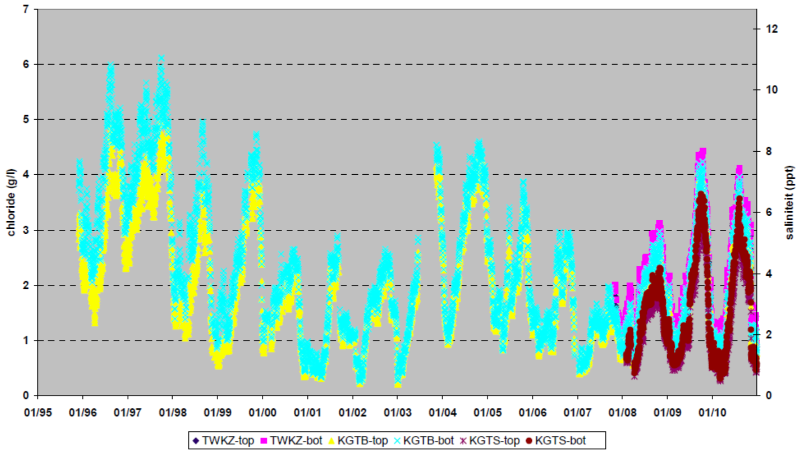

FIGURE 3-4. HISTORIC SALNITY CONCENTRATIONS IN THE GTC, CONSISTENT FOR THREE STATIONS OVER PERIOD 2007-2011 (VANDERKIMPEN ET AL., 2012).

.All data, for the listed stations, appears complete from the end of 2007 onwards, therefore the model is verified for 2 representative salinization years, respectively 2010 and 2011. The peak of the salinization in 2010 is fairly average and the salinity concentration comply within the prescribed water quality standards in the treaty. The year 2011 shows the highest salinization over the past decade, the levels measured at KGTS station for a period of several months is far beyond the limit of 5.8 ppt, over two months averaged.

Although the salinity measurements are given for top and bottom, suggesting near surface and near bed level, sensors monitor salinity levels are positioned at a vertical reference level of +1.00 m and -5.00 m +NAP, whilst the average bed level in the middle of the canal is -11.5 m +NAP. This most likely means that the bottom salinity is underestimated. The bottom salinity from the LMC gives a conservative image compared to the original data from two monthly salinity measurements by HMCZ over 11 points in the GTC. After all, the longitudinal salt profiles visualized in Appendix III. Longtudinal Salt profiles gave rise to further research into salt intrusion with the emphasis towards the impact of density driven salinity transport. For each point, salinity is measured with depth intervals of circa 1 m. The vertical salinity gradient is more or less invisible in the high frequency data as shown in Figure 3-4. However, the salinity at the surface proves to agree really well and so they are considered to be very reliable, especially since one of the two data sources is measured with high-frequency. This data is the best available to verify the model performance. The two monthly salinity will be used to estimate the stratification. The difference between the near surface and near bottom salinity is limited to around 1.5 ppt. However, horizontal patterns in the salt profiles demonstrate that the vertical salinity gradients are larger. In the time series, the variety in the vertical salinity distribution is still fairly limited but during dry summers these differences can increase up to 4 ppt near the locks. The longitudinal salinity observations, from 11 impermanent measuring locations, shows that over the horizontal plane the top half of the water column is vertically uniform or well-mixed (Appendix III). The bottom half covers the salt wedge, so here salinity shows a faster incline over the depth. It implies that the high frequency bottom salinity in Figure 3-4 was measured in the well-mixed zone. Wind forcing influences the free surface and the uniform vertical distribution in the top half is likely caused by passing ships. Unlike in shallow canals, these mixing effects caused by boat propellers apparently do not reach all the way down to the bottom (Lebbe, 2009); (Steenkamp et al., 2004).

The characteristics of the salt intrusion in the GTC, shows that the salinity is quite resilient to high discharges. Several days of high discharge leads to stagnation of the salt intrusion, but for substantially lowering salinity levels, a longer period of high discharge is needed. Unfortunately, there are no measurements conducted in the GTC into the flow velocities, so this cannot be used in the calibration of the model. If the vertical profile of the horizontal velocity is not close to a logarithmic profile due to stratification, it will prove once more that density driven flows are important and a 3D-model for the transport of matter is recommended.

4 MODEL SETUP

This chapter describes what methods are applied to schematize the GTC system and how the model boundaries, initial conditions and parameters for Delft3D FM salinity model are imposed. Prior to the setup, the physical processes behind the new generation hydro software are explained.

4.1 Modelling Software

All modelling is done using the Delft3DFlexible Mesh software that has recently been launched (Donchyts et al., 2014). For this study, both the standalone beta version of Delft3DFM and the plugin version integrated in the Delta shell framework were applied. The graphical user interface developed within the Delta shell project is extensively integrated with GIS technologies. This played an important role in the data preparation and presentation, unfortunately some 3D features were not supported at the moment the study took place. Therefore, 3D computations were computed with a standalone version, capable of simulating the required boundary conditions.

The name ‘Flexible Mesh’ refers to the flexible combination of rectilinear or curvilinear grids and unstructured grids composed of triangles, quads a rectilinear or a curvilinear, boundary fitted grids (Donchyts et al., 2014). The new computational core essentially computes faster and allows more accurate flow estimations. Furthermore, the software shares many similarities with its predecessor Delft3D. In principle it solves the same equations, uses similar theories and the methods of defining boundaries have the same roots, but different numerical grids or meshes are used. Still, the change in grid is not the only difference. The numerical discretization, used to solve the equations of motions, have been updated for the curvilinear grids as well. Besides all these new advantages, several other discretization methods have been introduced in the software.

The Delft3DFM program is in continuous development and not all features have been fully tested yet. Santosa et al. (2014) showed encouraging results with their Delft3D-FM salinity model of the Colombia estuary, which spatial scales are much larger than in the current study. The hydrodynamic module Delft3DFM simulates 2DH (depth-averaged), or 3D unsteady flow and transport of matter resulting from tidal and/or meteorological forcing, including the effect of density differences due to a non-uniform temperature and salinity distribution (Deltares, 2016). It aims to model the flow phenomena, the horizontal length and time scales of these are significantly larger than the vertical scales (hydrostatic pressure assumption). Besides the Delft3DFM software, several pre- and post-processing tools were used. Processing the model output was mainly done in MATLAB version 2015b and Excel. The Quick plot extension within MALTAB offered the opportunity to get a quick and effective first impression of the output.

4.2 Hydrodynamics and Transport of Matter

The governing equations in hydrodynamics and the transport of matter are elaborated in general terms. The way of discretizing and solving the flow equations, vary by the model but the hydrodynamics and the transport of matter are based on the same theories. The complete set of equations can be found in the Delft3DFM user manual .

Delft3DFM solves the unsteady shallow water equations in two or in three dimensions. These equations are derived from the three dimensional Navier-Stokes equations for incompressible free surface flow. Also, the Boussinesq estimation is used, which means the effect of variable density is only taken into account in the pressure term. The transport of matter and heat is modelled by an advection-diffusion equation in three co-ordinate directions. Advection, dispersion and diffusion are the flow processes that explain the transport of salinity in surface waters (Steenkamp, 2004). Transport by advection in either the vertical or horizontal direction is caused by the movement of water. The diffusion of salinity happens because of the concentration differences in water layers, this type of transport is considered to be very limited, because it happens over longer timescales. Dispersion is the redistribution of momentum and matter due to the vertical variation of the horizontal velocity. Dispersive transport is assumed to be the dominant process and the type by which saline density flows are denoted.

The set of partial differential equations, combined with an appropriate set of initial and boundary conditions is solved on a finite difference grid. Delft3DFM applies a finite volume solver on a staggered grid, meaning that not all quantities, such as; the water level, the depth, the velocity components or concentration of substances are defined at the same location in the numerical grid. However, there is no concept of grid 'rows' and 'columns' and the continuity equation is solved implicitly for all points in a single combined system. The time integration is done implicitly on all term except for the advection term. The latter is done explicitly, the resulting dynamic time-step limitation is automatically set based on the Courant criterion. The possible performance downfall using this approach, can be remedied by refining and coarsening the computational grid in the appropriate locations (Deltares, 2016). The grid size is usually too coarse and the time step too large to resolve the turbulent motion scales in numerical models. Thus, turbulent processes are added "sub-grid" using a turbulence closure model. In addition to all turbulence closure models in Delft3DFM, a tempo-and spatial constant ambient mixing coefficient is user specified, based on the concept of eddy viscosity (Deltares, 2016).

4.3 Model Schematization

4.3.1 Mesh generation

A major issue is the level of detail required to model long-term salinity transport. Highly resolved 3D simulations are computationally very demanding. Therefore, generally compromises have to be made in the modelling approach, between the mesh resolution, the user time step and the overall runtime of the model. No similar model schematization was available of the GTC salinization studies, therefore the mesh had to be constructed from scratch. Mesh quality is critical to the accuracy of simulations and interlinked to the preferable computing time step, so the resolution along the domain had to carefully though of during the mesh generation. Numerical modelling also implies paying attention to other factors like the quality of input data, the desired quality of the output and of course the quality of comparison data. he most important design criteria used for the mesh are:

- Meet accuracy and quality standards
- Ensure sufficient coverage of density gradients
- Workable simulation time

Accuracy and quality standards are defined in the Delft3DFM user manual. For curvilinear grids, orthogonality is required to minimalize the numerical errors during simulations. Orthogonality means that for each grid cell, the two lines drawn from the adjoining, opposite grid cell centres must intersect the cell face (nearly) perpendicular. Across the entire mesh, the orthogonality was kept internally below 1% and along harbour connections within 3%. These values lie within the advised range set within the user manual (Deltares, 2016). By default, a width-length ratio of 0.8 or 1.2 is prescribed to create a smooth transition between adjacent mesh cells. Because the flow in the GTC is predominantly in a longitudinal direction, a deviating width/length ratio was chosen. The entire mesh could have been created using unstructured mesh cells. However, the practical use of curvilinear grids in combination with flexible unstructured connections made it convenient to apply rectangular mesh cells for the main channel rather than a fully unstructured mesh with triangles and hexagons. The horizontal mesh is illustrated in Figure 4-1 and contains 3629 grid elements and 4199 corner nodes.

Lateral grid spacing dynamically varies between 30-45 m. Influences of transverse flows on the salt distribution are considered negligible, therefore lateral spacing was kept high as possible. However, a minimal number of width cells are needed to implement cross-sectional bed variations. Longitudinally the grid spacing varies between 50-100 m, to acquire a smooth transition between the main channel and the harbours and the channels towards the locks, local mesh refinements are applied (Figure 4-1, Detail 1). With the available resources for the research a calculation time of 1 to 2 days is acceptable.

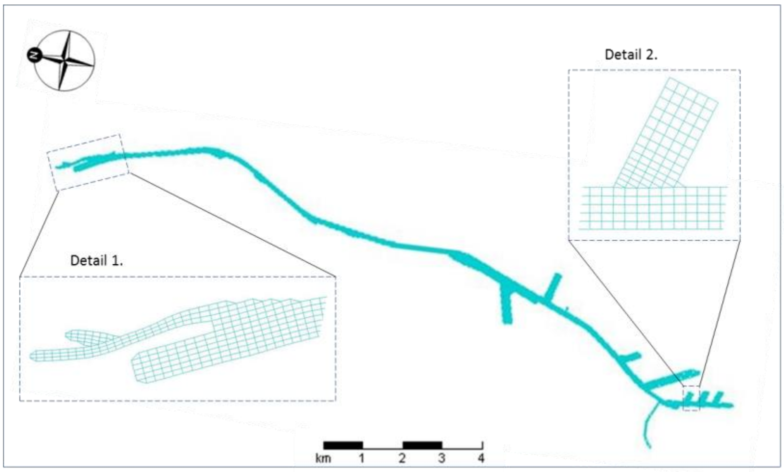

FIGURE 4-1. DELFT3DFM MESH OF THE GTC MODEL. THE NUMERICAL GRID IS MAGNIFIED IN DETAIL 1 (NEAR THE TERNEUZEN LOCK COMPLEX) AND DETAIL 2 (THE 'NOORDDOK' IN GHENT).

The mesh contains a curvilinear grid covering the main channel, individual grids of the various harbours and unstructured connection. The curvilinear approach offered the efficiency and effectiveness to schematize the hydraulic surface area, whereas unstructured mesh links provided the desired flexibility to mount branches (Figure 4-1, Detail 2).

4.3.2 Layer model application

In the vertical direction it offers two different vertical grid systems, each with their own range of applications. Both systems are illustrated in Figure 4-2:

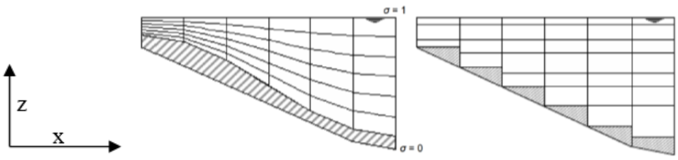

FIGURE 4-2. LEFT). SIGMA LAYER MODEL, RIGHT). Z-LAYER MODEL (DELTARES, 2016).

Within the sigma-layer model, the number of vertical layers over the entire horizontal computational area is constant, irrespective of the water depth. A smooth representation of the topography is obtained. Both the moving free surface and the bed follow the horizontal coordinate lines. The z-layer is not boundary fitted in the vertical plane. The number of layers is dependent on the depth of water. The layers are strictly horizontal and create a staircase representation of the bed. The mayor advantage of the z-model is that the horizontal grid lines are parallel with density interfaces (isopycnals) in regions with steep bed slopes. This is not a strict requirement but it is a welcome aspect as it helps to reduce the artificial mixing of scalar properties like salinity (Deltares, 2016). The z – layer model will provide the best fit, however it had recently been implemented and its functionality is not tested thoroughly. Applying the sigma layer model will give comparable results as the layer conditions are similar to those in the z-model. The coordinate lines are in fact horizontal for the largest part of the domain, similar to the z-model. The function 'Anti-creep' deployed in the sigma model (Sigma AC), suppresses artificial errors that lead to artificial mixing. The GTC's bed topography only shows some local bed variations near the lock complex, the influences are likely very local but may have an significant effect on the simulated salinity. Essentially, this option allows the application of a third layer model which has the advantages of both the regular z-and sigma model. Sigma AC is used in this thesis, however it is estimated that anti-creep computation time for this layer model is 1.5 times longer (Deltares, 2016). The layer distribution can be set to non-equidistant, allowing more resolution in the zones of interest.

The vertical resolution is derived by the statement of Ballegooyen et al. (2004), who found that the minimum number of layers required to adequately simulate vertical stratification, must be larger or equal to the largest vertical salinity gradient over the entire spatial domain. The maximum gradient is rate of change in salinity per unit of depth. Section 3.3 denoted that the gradient near the locks is max 4 ppt. Therefore, 5 layers would be sufficient. However, this gradient is likely to increase due to the new lock changes and thus 10 layers are chosen.

4.3.3 Bathymetry

In 2012, RWS *Zee & Delta* in cooperation with the Flemish Hydraulic Research Centre situated Antwerp, performed the most recent bathymetric sampling for the entire channel. These high resolution depth samples are processed into a geographical information database named Baseline, which is an extension within the ArcGIS environment.

For the entire domain, the density of the sampling data is much higher than the density of the mesh and therefore an accurate representation of the bathymetry can be obtained. To project sampling data onto the network nodes, Baseline applies a pointwise approach rather than an averaging technique of multiple nearest depth samples. In principle, the closest sampling value will be awarded to a network node, which is either bed level or embankment level. Thus upon the nodes that constitute the outer contours of the mesh, bottom bed heights were projected and not the actual height of the embankments. Delft3DFM features many conveyance types to reflect various projection types of the bed surface, however the correct and most accurate bathymetry is obtained with the default setting in combination with manual adaptations of the outer network nodes. The final GTC models bathymetry is displayed in Figure 4-3.

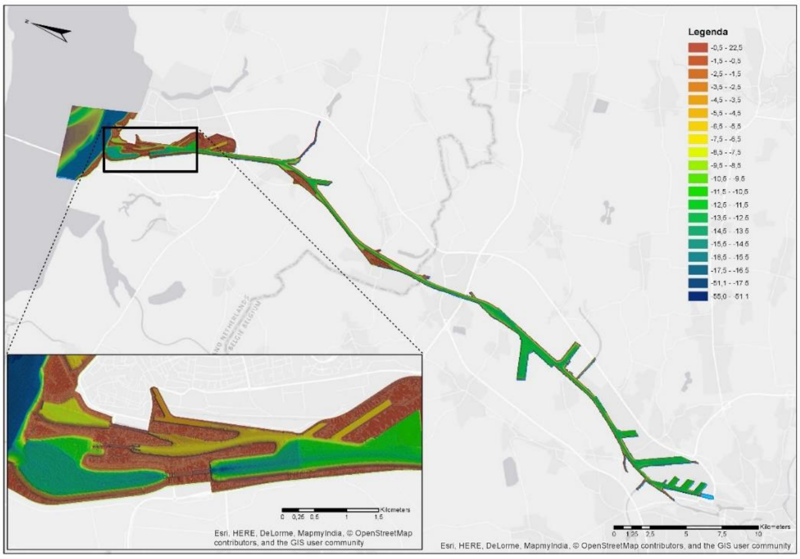

FIGURE 4-3. LEFT). DETAIL OF THE BATHYMETRY NEAR THE LOCKS . RIGHT). THE OVERALL GTC BATHYMETRY IN 2012

4.4 Boundary Conditions

4.4.1 Upstream boundaries

Applying the most appropriate and correct boundary conditions to the GTC model turned out to be challenging and the most important assignment in the model setup. The model input is already described in section 3.2.1 and 3.2.2, and therefore only the schematisation methods are described. Two open discharge boundaries are imposed in the southern part of the domain with homogeneous salinity constituents. At Evergem, freshwater is fed to the GTC via the Ringvaart and five km in downstream direction the Moervaart discharges water in the channel. No profound discharge and salinity data were available thus the imposed inflow was estimated based on the total outflow via the locks, with an discharge ratio of 0.88 Ringvaart and 0.12 Moervaart (Section 3.2.2). Imperfections in this distribution will be interpreted and discussed in the model results. Salinity constituents of the two inflows determine the background concentration in the GTC. As no data was found for these streams the assumption was made that the Ringvaart and Moervaart are freshwater inflows. This assumption implies that salinity for freshwater basins like the Moervaart and the Ringvaart is around 0.5 ppt, the latter value was adopted as salinity constituents.

4.4.2 Downstream Boundaries

The downstream boundaries consists of three branches connecting the main channel toward the locks, where control structures are used to control the discharge fluxes in-out of the domain. A schematic 2DV section is shown in Figure 4-4 to indicate how the sinks and sources are imposed.

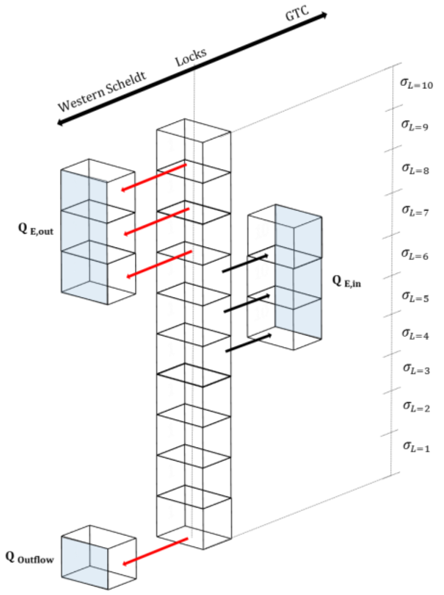

FIGURE 4-4. SCHEMATIC VERTICAL DISTRIBUTION OF SINKS AND SOURCES, CONTROLLING THE FLUXES IN-OUT THE DOMAIN.

The channel is modelled with sufficient detail, but the mixing processes near the locks cannot be resolved by open discharge boundaries. Therefore, a complex vertical distribution of sources and sinks is applied, resulting in three different discharge fluxes. The schematization of the boundaries, at every branch towards the Western, Middle and Eastern locks is different, but the principle is still in line. Depending on the estimated thickness of the discharge fluxes, water is discharged through one or more cells. Alternative methods, to extract flows on closed model boundaries by adding or withdrawing water from a layer, for example with culverts, are currently not available in Delft3D FM.

The schematic representation in Figure 4-4 is applied for the Middle and Western Locks. It slightly differs from the schematisation of the Eastern Lock, here the outflow of the GTC is withdrawn from the surface layer ($\sigma_{L=10}$). instead of the bottom layer ($\sigma_{L=1}$). The Eastern lock discharges water through levelling valves in the lock doors, and not by culverts. The $Q_{outflow}$ is the average daily outflow of the locks, consisting of levelling losses and the drained volumes to control the water level. For all locks the outflow is withdrawn from a single cell. Figure 4-5 shows the time series of the lock outflows over the period 2010-2011. This period is selected as the model will be calibrated and validated on these conditions.

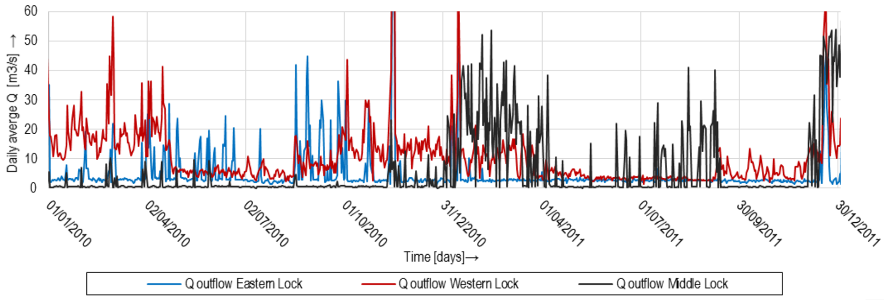

FIGURE 4-5. HISTORIC LOCK OUTFLOWS 2010-2011.

The density flows in-out the model domain $Q_{E,in}$ & $Q_{E,out,}$ that occur during lock operations are distributed over multiple vertical layers. In general, the freshwater flux or plume is extracted from the three highest vertical layers ($\sigma_{L=10,9,8}$), the saltwater influx in the channel is discharged deeper ($\sigma_{L=7,6,5}$). The water depth in the individual locks is however the decisive factor for the number of cells over which the fluxes are divided, because in the vertical plane above the lock bottom the exchange process takes place. Due to the depth differences in front of the locks the thickness of the sigma layers varies for each lock branch. The product of exchange flux is zero at all time as the withdrawal and intake of water are equal. This assumption had been made in the estimation of the exchange flows (Section 3.2.3). Applying the z-layer model would have not have led to layer differences in the lock schematisations.

The fresh-saline fluxes over the model boundaries are imposed by pre-defined time series on sinks and sources, based on estimations of the exchange per lock. All flow and salinity conditions of the exchange flows were mentioned in Section 3.2.3. It is noteworthy that the product of these fluxes, over a large part of the time series, is larger than the freshwater inflow. In Chapter 5 it is determined whether a scaling of these values is required. The $Q_{E,in}$ & $Q_{E,out,}$ are imposed as constant values in time, saltwater discharge flux continuously enter the channel and simultaneously an equivalent (brackish) fluxes leaves the domain. The depth average salinity concentrations measured in the outer port in the Western Scheldt are used for the salinity constituent of the $Q_{E,in}$. The salinity constituent of $Q_{E,out}$ is calculated by the Delft3D FM model.

The water inflow via the upper boundaries and the combined outflow through the sinks is aligned to control the water balance and to maintain a constant water level. Small differences are not allowed, over time, they will result in an incorrect water balance and the model runs empty. Modelling with sources and sinks in Delft3D FM can only be done with time-series, and cannot be done on the basis of imposed conditions that depend on simulated hydrodynamic variables, so that the outflow is calculated automatically. The management of the outflow via the locks, as described in Section 2.2.1, can then easily be integrated and will make the model more user friendly and better operable. Currently, inconveniences occur when creating future scenarios. The impact of lock modifications will be assessed with historic flow regimes, therefore this does not results in problems in the scenario analysis.

4.5 Initial Conditions

In order to keep the warm up period in the simulations as short as possible, appropriate initial conditions (IC) have been adopted for the water level and the salinity. The initial water level is straight forward as the level is controlled at the virtually stable value of 2.13 + NAP. In reality, a surface slope of a few centimetres is observed over the domain, however this is not included in the simulation as this is not possible with the selected schematisation methods of the boundaries. Setting the initial salinity field is more complicated, since the horizontal and vertical distribution varies over time. The application of spatially varying salinity fields was considered. However, Delft3D FM only supports horizontal salinity fields over with a linear interpolation between the surface and bottom layers (Deltares, 2016). Running the model with an uniform salinity field over a warming period resulted in similar initial conditions with less effort. Therefore, all simulations start and end in the winter as the vertical and horizontal salt profile is most uniform in this period. The warm-up period in combination with a spatially uniform salinity allows for a reasonable distribution and salinity balance at the beginning of all simulations.

4.6 Physical Parameters and Model Constants

The gravitational acceleration constant is 9.81 m/s^2. Delft3D FM requires a background value for the water density, but this value is only used for homogeneous simulations, which means that the temperature and or salinity modules are not selected. For the GTC model the salinity module is selected, therefore a default water density of 1002 kg/m^3 has been adopted, although the actual water density is computed by the model. Temperature gradients and wind stresses on the free moving surfaces are not accounted for in the simulations.

Roughness formulation

For 3D models, Delft3DFM uses a quadratic bed stress formulation that is quite similar to depth-averaged computations (Deltares, 2016). Overall, little knowledge about the systems roughness coefficients was at hand, thus a well-founded approximation had to be made based on values used in similar studies (Lebbe, 2009). In order to compute the bottom roughness, based on the local bed stresses, the Manning formula was applied with n = 0.023 s/m$^{1/3}$. The influence of this parameter on the model's salinity performance will be tested during the model calibration.

Flow parameters

The two model parameters, the horizontal eddy viscosity [HEV] and horizontal eddy diffusivity [HED], affect the horizontal movement of the flow and transport of matter are based on the general eddy viscosity concept. For both parameters a spatial uniform ambient values of 1 m^2/s is used. In general, eddy viscosity is a function of time and space, and the size of these parameters is therefore also different for different mesh resolutions.

Turbulence parameters

In Delft3D FM, the 3D turbulent eddies are bounded by the depth of water. Their contribution to the vertical exchange of horizontal momentum and mass is modelled through a vertical eddy viscosity [VEV] and eddy diffusivity coefficient [VED]. The k-ε turbulence model computes the mixing length based on the VEV, VED and ambient values. The coefficients are assumed to be proportional to a velocity scale and a length scale (Deltares, 2016). With both parameters, the mixing effect of shipping can be included, if the model has a tendency to overestimate stratification. Initially, spatial uniform ambient values of 5e^{-5} m^2/s are used for the VEV and VED. Optimal values will be derived in the calibration process.

Time setting

Estimating the model simulation time and computational performance is difficult. Preferably a single year simulation should run over one night, applying parallelization over multiple cores. In theory, a dynamic user time step of 10 minutes maximum satisfies the numerical stability criteria for the entire mesh, but this step is the coarse for the modelled sinks ($Q_{outflow}$). Pre-defined sources and sinks are treated explicitly in the numerical scheme. Thus, the time step is not updated according to the stability criteria, like Delft3D FM does for the mesh. Instead the discharge of the sink cell is limited, based on the courant velocity criterion [CVC]. From this, the maximum time step is calculated, unfortunately this step is unnecessarily small throughout the simulation period. The water balance should be fitting otherwise the model cannot correct this anymore. The $Q_{outflow}$ via the Eastern lock proved to be the limiting factor under extremely high discharges. The estimated layer sigma thickness at the Eastern lock is only 0.85 m, but simply dividing the outflow over more cells is not straightforward, the resulting fixed user time step is:

$$\Delta t \leq \frac{C_{velocity} \times V_{sink\ cell}}{Q_{max}} \qquad \Delta t \leq 6.9\ s \qquad \text{EQUATION 2).}$$

Δt	=	Maximum user timestep	$[s]$
V $_{sink\ cell}$	=	Volume of the local sinkcell	$[\mathrm{m}^3]$
Q_{max}	=	Maximum discharge through cell is 75	$[\mathrm{m}^3/\mathrm{s}]$
$C_{velocity}$	=	Courant velocity criterion value is 0.7	$[-]$

5 CALIBRATION & VALIDATION

An impression of the model performance with the initial parameters settings is given to demonstrate the flow processes near the locks. In sequel, an assessment with parameter variations will be presented to determine how sensitive the salinity levels are for parameter changes. The ability of the model to simulate historic salinity dynamics in the GTC is evaluated for a calibration period (2011) and validation period (2010). The optimized parameter set is derived during the calibration procedure.

5.1 Initial Model Results

The required computational capacity cannot be obtained by a single computer. Parallelization was used for faster computations on shared or distributed-memory machines. The time settings used in the simulations with the initial parameter settings are shown for a full simulation year in Table 6. The years 2010 and 2011 were chosen for the calibration and validation periods, both runs are preceded by a spin-up period of 15 days.

TABLE 6. TIME SETTINGS.

Model	Simulation time	Cores	Grid elements	Time step
[type]	[hour]	[number]	[number]	[s]
Delft3D FM	about 28	18	3629	6

Prior to 3D simulations, it is common practice to run the model with only one layer (2DH). This implies a depth average calculation in which the functionality of the model boundaries can be verified and possible errors can be identified easily and therefore dealt with in a time efficient manner. However, this practice is not possible because the exchange flows are explicitly imposed since the sources and sinks are placed on top of each other and this cannot be performed in a single layer sigma-model.

The initial run, over a period of the first 100 days in the year 2011 showed an unrealistic salt balance. Inflowing saltwater fluxes were not in proportion to the outgoing fluxes at the locks. As a result, saline water accumulated near the downstream boundaries, creating unrealistic flow patterns caused by the density driven flows in direction of Ghent. Such behaviour near the locks, causing the horizontal flow direction to alter over the full water depth is not supported by measurements. The two monthly salinity measurements proccessed into longtudinal salt profiles, indicates that the saltwedge on the bottom of the GTC always strechtes a few km inland, but at the start of the annual salization cycle in January, it is at its smallest. The saltwedge starts moving upstream when the freshwater inflow rate in Flanders drops in summer.

At the start of this thesis it was not the intension, but the explicitly imposed lock exchange flows needed to be lowered to gain satisfactory model results. Within the current possibilities to schematize, it appears unfeasible to integrate the efficiency of the saltwater reducing systems over the downstream boundaries. As a result, the different exchange ratios per lock required a uniform downscaling to 21% of the initial exchange ratios this corresponds with fresh-saline discharge fluxes of 4.86 m^3/s of the Western lock, 0.5 m^3/s of the Middle lock, and 0.61 m^3/s at the East lock, constant over time.

The water density and flow velocity are indicators to demonstrated that the results comply with the observed behaviour of the salt wedge. The horizontal water density fields including velocity vectors show the flow patterns and direction of the flow in Figure 5-1 and Figure 5-2. The results are taken from the bottom layer $\sigma_{L=1}$ and the surface layer $\sigma_{L=10}$, at the start of the annual salinization cycle and at the beginning of summer.

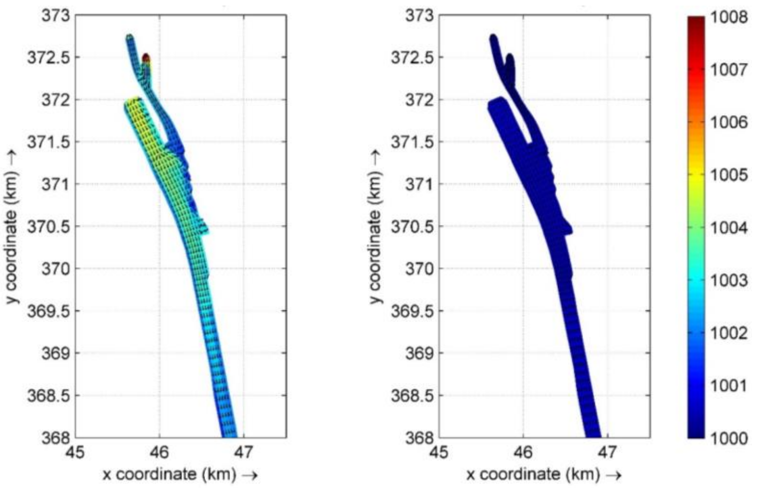

FIGURE 5-1. WATER DENSITY FIELDS INCLUDING NORMALIZED VELOCITY VECTORS AT 01/01/2011.
LEFT) BOTTOM LAYER $\sigma_{L=1}$; RIGHT) SURFACE LAYER $\sigma_{L=10}$.

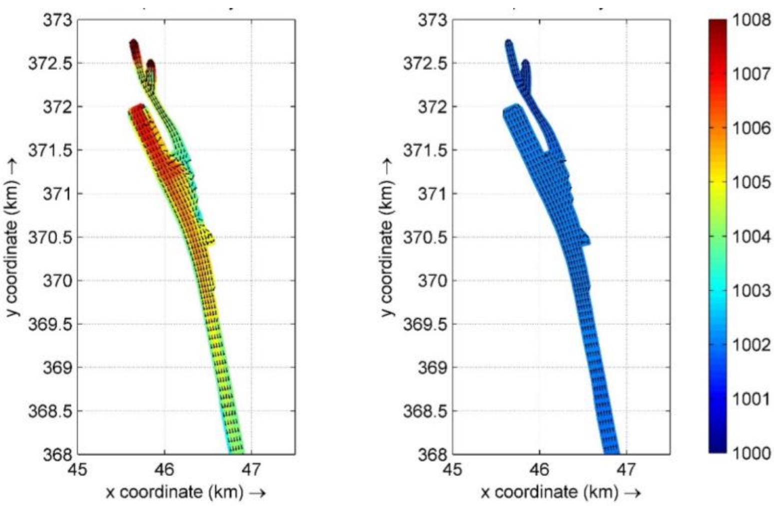

FIGURE 5-2. WATER DENSITY FIELDS INCLUDING NORMALIZED VELOCITY VECTORS. 15/04/2011.
LEFT) BOTTOM LAYER $\sigma_{L=1}$; RIGHT) SURFACE LAYER $\sigma_{L=10}$.

The simulated internal vertical flow velocities over the horizontal domain confirm an alternating flow direction between surface and bottom. The higher density near the bottom shows that the salinity is larger at the bottom, referring to the accumulation of saltwater in front of the locks. More than three months after the start of the annual salinization cycle, the salinity distribtion changes in the domain, the saltwedge starts migrating the direction of Ghent, primaily in the bottom layers (left Figure 5-2). The difference between the bottom salinity, January 1th and April 15th elucidates that saltwedge streches further inland. Over time the higher water layers will gradually follow, increasing the salinity in the surface layer as well. (Right Figure 5-2). The comparion between the surface and bottom salinity in Figure 5-1 and Figure 5-2 demonstrates that the complex lock schematization method of sinks and sources functions well.

5.2 Sensitivity Analysis

In the sensitivity analysis, the influences of the bottom roughness, the horizontal eddy diffusivity [HED] and the vertical eddy diffusivity [VED], on the salinity dynamics are assessed. The differences between the default values, applied in the initial model run, and a carefully selected parameter range are assessed. Knowing how large these influences are on the behaviour of salinity will help to determine the optimal parameter settings. The GTC model is a small scale model, therefore is assumed that the influences of boundary forcing will be significant throughout the domain. Station KGTS, located at the Dutch-Flemish border, is the furthest observation point away from the model boundaries and is selected to examine the salinity deviations due to parameter variations. The influence of the boundaries is minimal at this location and the changes in salinity levels due to unilateral parameter changes will is the best noticeable. In this section, salinity changes at the surface as well as the bottom are evaluated on a qualitative basis. Appendix IV holds all the results of various simulations in the sensitivity analysis.

Bottom Roughness

The roughness coefficient affects the flow resistance or the shear stress over the modelled domain and plays an important role in the verification of the hydrodynamics. The magnitude of the bed shear stress is characterised by means of the roughness coefficient, which is of the type manning. Based on this *n* value and the local water depth, local Chézy roughness values are computed. The average water depth is quite consistent throughout the domain and fluctuates between 11-13 m. Thus the computed bottom roughness is constant over time but shows small lateral variations. A realistic range of *n* between 0.020, 0.023 and 0.026 s/m$^{1/3}$ is selected, based on the user manual and corresponds to rather smooth bed surfaces (Deltares, 2015). The suggested upper limit is already quite rough. Appendix IV shows that the parameter appears to have an negligible effect on the surface as well as the bottom salinity levels and the vertical salinity distribution.

Horizontal Eddy Diffusivity [HED]

The diffuse term of the salinity transport is dependent on the HED. Horizontal eddies are assumed to be of more importance in small scale models where its effects are more significant. (Deltares, 2015). This parameter is space and time-dependent and so naturally a larger time step means a higher value for the HED is needed, based on the selected mesh resolution. Appendix IV. Sensitivity Analysis shows the variation of the bottom and surface salinity by change in the HEV coefficient. Using the Delft3D FM user manual and with advise of consultants at Deltares, a realistic parameter range is selected by increasing and decreasing the default values with a factor of 10. By default, the ambient value is 1 m^2/s. A decrease of this parameter, by a factor 10, ensures a small reduction in the stratification. An increase of this parameter by a factor of 10, compared to the default, has a negligible influence on the salinity.

Vertical Eddy Diffusivity [VED]

In general, the value of VED is a number of times lower than the HEV value. The turbulence model calculates the turbulent eddies for every time step, based on the ambient value. Vertical mixing in the top of the water column is caused by the movement of vessels. It is an important physical processes that partially defines the vertical salinity distribution in the GTC is. Selecting a higher ambient value for the VED enlarges the turbulent eddies in the domain, therefore the VED coefficient can compensate for the mixing effect caused by ships, but it effects the turbulent eddies over the whole depth. The advised range for the VED, in small-scale simulations like the GTC system, lies between 0 and $5e^{-6}$ m^2/s according to the Delft3D and Delft3D FM user manuals. For highly stratified flows, it is suggested to apply an ambient or background vertical eddy viscosity in the order of $10e^{-4}$ m^2/s for the vertical exchange of momentum. This value corresponds with field measurements in the Rotterdam Waterway, The Netherlands (Deltares, 2015). By default the VED value in Delft3D FM is $5e^{-5}$ m^2/s and simulations with a factor 10 higher show that the model reacts highly sensitive to changes in this parameter (Appendix IV). The variance in the vertical salinity distribution at this location rises and the surface salinity shows little change in comparison to the default value. The bottom salinity is clearly affected, because the stratification in the domain becomes larger, however total salt balance in the model is lower. A factor 10 decrease, shows that the stratification lowers, the impact will cause less changes in the vertical salinity concentrations compared to an increase of this parameter.

5.3 Visual Comparisons

The model calibration and validation is carried out for multiple periods. The year 2011 is selected because the decades highest salinity levels were recorded in this year. With perspective to construction of the new lock, the model must be able to reproduce these high saline conditions accurately. For the period 2010, moderate salinity levels were recorded. Accurately simulating the different annual salt intrusion cycles over the years 2010-2011 with the same parameter settings will prove the models ability in reproducing salinity dynamics in the GTC. This reduces the amount of uncertainties in scenario analysis and provides confidence that physical processes are correctly embedded in the model.

Ideally the calibration process includes a hydrodynamic calibration and validation as well, but there were no flow velocity data available. Furthermore, the GTC model maintains a constant water level so verification of this variable is not possible. Great modelling efforts were put in the translation of the high resolution bottom data onto the numerical grid and realistic variations of the bottom roughness parameter proved to have an insignificant effect on the salinity dynamics. Therefore, further optimization of the bathymetry proved to be irrelevant. The model fit for the surface and bottom salinity were optimized by fitting the horizontal and vertical eddy diffusivity coefficients. The optimized lock exchange flows had been defined in Section 5.1.

Relating to the default parameter values, the setting is only slightly changed because the general salinity trends and the stratification in the domain were already fairly well reproduced with the default parameter settings and the scaled lock exchange flows. As a result of the calibration and validation procedure, the following optimum values had been set for the manning roughness (0.023 $s/m^{1/3}$), the VED ($4x10^{-5}$ m^2/s), HED (0.1 m^2/s). As recommended by Deltares, the vertical eddy viscosity VEV ($5x10^{-5}$ m^2/s), and horizontal eddy viscosity HEV (1 m^2/s) were left default.

The Delft3D FM salinity results and measurements of the both the calibration and validation period are visualized in Figure 5-3 up to Figure 5-6 along with the salinity from two data sources. The simulated bottom and surface salinity respectively are taken from the bottom ($\sigma_{L=1}$) and top layer

($\sigma_{L=10}$). Station TWKZ records salinity 500 meters upstream of the Western lock, Station KGTB at Sluiskil (3.5 km upstream) and station KGTS at Sas van Ghent (10 km upstream) and VMM1 ($\pm$ 25 km). Green lines show the simulated surface salinity concentrations. Grey lines represent the observed surface salinity [ZEGE] whereas the red and green markers show the two monthly measurements of the [TSO] data base.

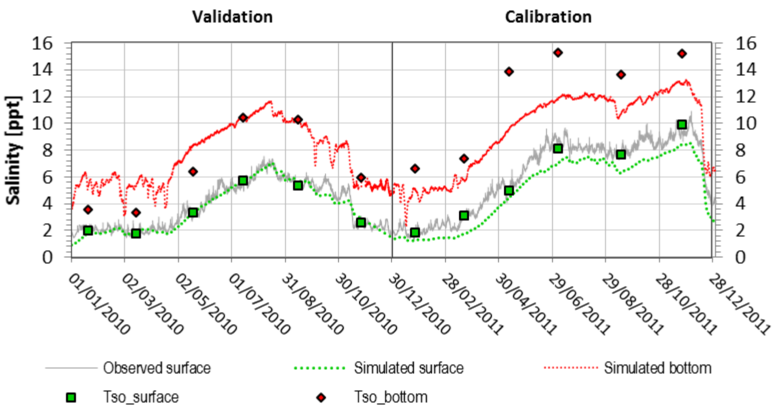

FIGURE 5-3. STATION TWKZ, OBSERVED AND SIMULATED BOTTOM AN SURFACE SALINITY 2010-2011.

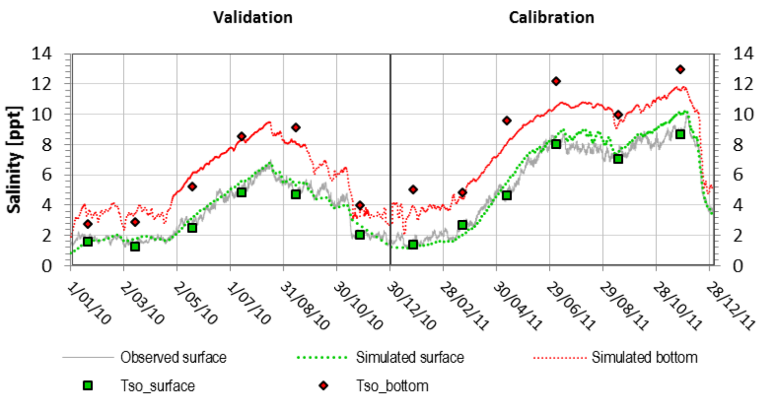

FIGURE 5-4. STATION KGTB, OBSERVED AND SIMULATED BOTTOM AND SURFACE SALINITY 2010-2011.

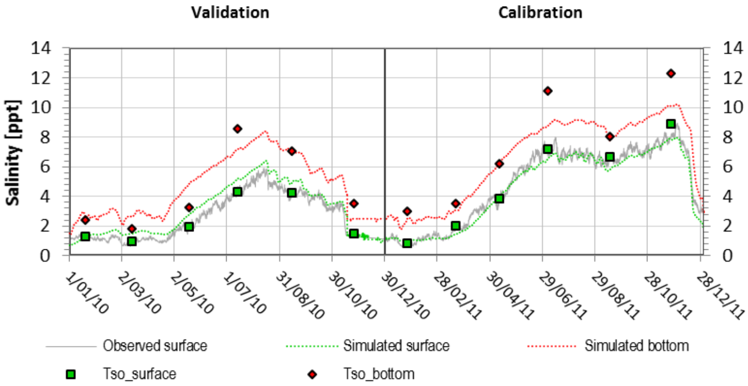

FIGURE 5-5. STATION KGTS, OBSERVED AND SIMULATED BOTTOM AND SURFACE SALINITY 2010-2011.

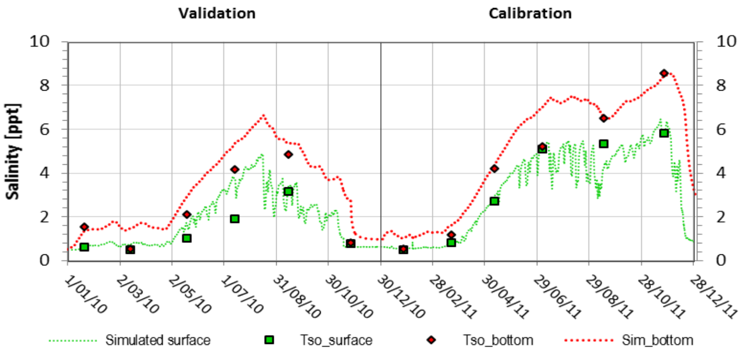

FIGURE 5-6. STATION VVM1, OBSERVED AND SIMULATED BOTTOM AND SURFACE SALINITY 2010-2011.

For stations VMM1, only periodic measurements are available and this locations contains valuable information about the reproduction of salinity levels far upstream. Therefore, a comparison is made with the two-monthly measurements.

Commented [bn1]: Goodness of the fit is almost perfect in the calibration year.

Validatie jaar bodem salinity bijna 1.5x zo hoog in de winter

5.4 Statistical Performance Indicators

Based on the data visualisations in the previous sections, the conclusion can be drawn that the model is able to reproduce salinity levels quite accurately over all stations. The surface salinity is reproduced somewhat better, though the at the bottom the data follows the few measurements reasonably. Along with the visual comparisons, the model performances were assessed by three statistical indicators. This comparison is limited to surface salinity, because the number of salinity measurements at the bottom is to limited to perform a statistical analysis with. Still, the few bottom salinity measurements were necessary to depict the overall stratification over the domain. The statistical indicators are the coefficient of determination (R^2), and root mean square error (RMSE) and the normalized root mean square error (NRMSE), the equations are listed on the next page.

$$R^2 = 1 - \frac{\sum_{i=1}^{n}(c_i - f_i)^2}{\sum_{i=1}^{n}(c_i - \bar{c})^2}$$ EQUATION 3).

$$RMSE = \sqrt{\frac{\sum_{i=1}^{n}(c_i - f_i)^2}{n}}$$ EQUATION 4).

$$NRMSE = \sqrt{\frac{RMSE}{c_{i,max} - c_{i,min}}}$$ EQUATION 5).

In which:

c_i = observed salinity
$c_{i,max}$ = maximum observed salinity
$c_{i,min}$ = minimum observed salinity
f_i = simulated salinity
n = number of values

The coefficient of determination calculation was applied to depict the variance of the simulated data compared to the measured data. Likewise, the root mean square error measure was also considered to quantify the error that is produced by the model in representing the observed salinity data. To depict the relative produced error the normalized root mean square error was computed. De statistical performance to reproduce observed surface salinity values is show in Table 7.

TABLE 7 STATISCAL PERFORMANCE INDICATORS OVER THE CALBRATION & VALIDATION PERIODS.

		TWKZ		KGTB		KGTS	
	Period	Cal	Val	Cal	Val	Cal	Val
R^2		0.80	0.94	0.94	0.94	0.97	0.84
RMSE in ppt		1.20	0.41	0.68	0.42	0.42	0.59
NRMSE		0.11	0.06	0.07	0.07	0.05	0.11

High R^2 values around 0.9 denote the strong linear association between the observed and the simulated surface salinity over all stations. Overall in the validation period salinity concentrations were reproduced better at the Stations TWKZ and KGTB, located in proximity of the locks. Over the calibration period the salinity concentrations could be reproduced better upstream in the domain. Evaluating the reproduced concentrations at station TWKZ, situated near the Western lock, the lowest R^2 and high error is computed here. Apparently, under high saline conditions the mixing processes near the lock cannot be fully reproduced by the model. A few km more upstream this error reduces already. Differences in the RMSE values between the calibration and validation year cannot directly be compared, because variance in the historic salinity records is higher in the calibration year. Therefore, the NRMSE show the relative model inaccuracy per station which appears quite high for the station TWKZ, but the NRMSE is at least as low or even better over the other two stations. Given the large number of assumptions, the amount of variables in estimating the exchange flows and uncertainties in the historic discharge data, the result is considered quite acceptable and estimated to be within the same range of the results in the EIA study. Although the periods used to calibrate and validate the model do not overlap and other methodology was applied. Moreover, it is questionable if the procedure in the EIA does not underestimate the depth average salinity levels in the GTC. In calibration of the Delft3D FM model optimized settings were derived using actual bottom salinity data, these data were not available for the calibration of the SOBEK 1D model. Therefore, the 3D GTC model produces higher salinity values when the output is converted to depth average values.

6 SCENARIO ANALYSIS

The scenario analysis assesses the changing salinity dynamics in the GTC caused by the planned lock modifications. The analysis is limited to a number of simulations with unilateral changes in the boundary conditions. Underlying assumptions, the applied salinity criteria and the results of the analysis are presented.

6.1 Salt Intrusion Scenarios

As has been highlighted in Chapter three, the repetitive annual salinization of the GTC caused by salt intrusion via the locks, is strongly influenced by the freshwater inflow from Flanders. The water shortage in low periods effects the ability of the Terneuzen system to flush back saline water, as the supplied freshwater is used for the levelling of the locks rather than using it for counteracting salt intrusion. From spring to summer, natural depressions in the inflow trigger the migration of the salt wedge in the direction of Ghent. The shortfalls in the supply and the duration of the low flow period determine the magnitude of the annual salt intrusion in the GTC. To assess the immediate consequences of lock modifications with the Delft3D FM model, the exchange flows ($Q_{E,in}$ & $Q_{E,out,}$) on one of the downstream boundaries will be enlarged. The seasonal freshwater inflow, as the most important variable, is varied over a number of simulations to compare salinity dynamics before and after instant lock modifications. Seasonal salinity differences are examined over the longitudinal profile of the GTC. The analysis encompassing six scenarios over a full simulation year, these are denoted in Figure 6-1 and will be briefly described hereafter. All scenarios are divided into two sets, the baseline set 'B' and the new set 'N'.

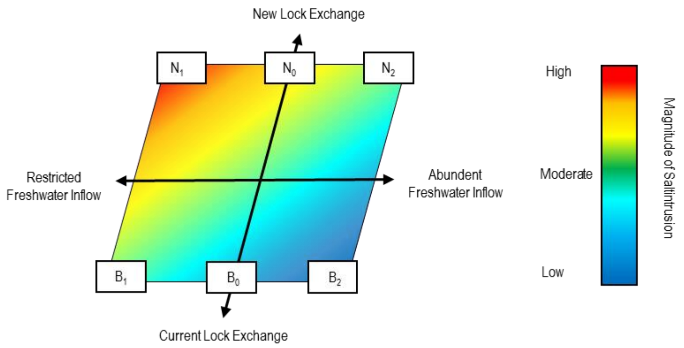

FIGURE 6-1. SUMMARY OF THE SIMULATED SCENARIOS.
IN THE BASELINE SCENARIOS B_1, B_0, B_2, THE CONSTANT EXCHANGE FLOWS OF THE CURRENT LOCKS AND THE INFLOW CONDITIONS OVER THE YEAR 2008, 2010 & 2011 ARE IMPOSED. AFTER ADOPTING THE IDENTICAL INFLOW CONDITIONS AND BY ENLARGING THE CONSTANT EXCHANGE FLOWS IN SCENARIOS N_1, N_0, N_2, THE FUTURE AND PRESENT SALINITY DYNAMICS IN THE GTC ARE MUTUALLY COMPARED.

The optimized parameter set, derived in the calibration procedure, is adopted along the initial uniform salinity and water level conditions. All scenarios are preceded by a spin-up period of 15 days to gain appropriate conditions at the start of the simulations.

In the new design of the Terneuzen port, the current Middle lock will be replaced by the new Sea lock at the exact same location. To accommodate the enormous lock into the current design of the inner port, the present land tongue between the Eastern and future entrance of the new lock will be removed. To complement the construction of the new lock, a separate sluice will be installed to discharge water. The installation of a separate sluice and the removal of the land tongue will be omitted in the schematization as the required mesh adaptations might bias the results of the scenario analyses. In Chapter 7 a discussion is held about the consequences of omitting several factors in the analysis.

6.1.1 Enlarging the exchange flows

Similar to the calibration procedure, per lock the exchange ratio is scaled to 21% percent of the initial estimated values (see Table 4 in the 6^{Th} column). The lock exchange flows applied in the simulations of the two sets of scenarios are shown in Table 8. In the new proposed lock situation, a significant increase in the cumulative salinity influx is observed. It is estimated that the total exchanged flux increases by a factor of 2.3 after the planned lock modifications are carried out. The salinity constituent for the exchange flows is composed from the average salinity difference between the GTC and the Western Scheldt, measured between the outer port of the Western Lock (Station TWZZ) and the inner port (Station TWKZ) and has a constant value of 22.6 ppt over time. Therefore, the long-term variations in the salinity levels of the Western Scheldt estuary do not influence the salinity concentrations in the new lock scenarios.

TABLE 8. LOCK EXCHANGE FLOWS.

Locks		B set	N set
		Exchange flows m^3/s	Exchange flows m^3/s
Eastern		0.61	0.61
Middle		0.5	-
Western		4.68	4.68
New		-	7.84
Total		**5.79**	**13.13**

6.1.2 Varying the freshwater inflow

In the time frame of the study it is not considered possible to predict the impact of the new lock under general flow conditions. In order to perform a comprehensive analysis of the annual salinization cycle, variations of the inflow per season need to be assessed, this will result in a wide range of simulations with constant flow rates. Therefore, the decision is made to impose the historical measured inflow of three decisive years, this time series also exhibits seasonal variations of the salinity cycle. The average inflow in the GTC is derived from the data in Figure 3-1 in Section 3.2, respectively for the periods from mid-Autumn till mid-Spring (Winter) and vice versa for the other six months (Summer). Table 9 presented on the next page, displays the historic average summer and winter inflow. The long-term winter and summer average inflow are used as comparative values to denote the freshwater availability in the selected scenarios.

Table 10 shows the average inflow over the three flow scenarios. For scenarios B_1 & N_1, similar to the calibration, the flow regime of 2011 is adopted. During this entire year, the supply of water was below average and the decades highest salinity levels in the GTC were measured over this period. For the year 2010, the winter and summer inflow was approximately average, the conditions are adopted in scenarios B_0 & N_0. The inflow into the GTC for the year 2008 is used in the scenarios B_1 & $N_{1,}$ the freshwater inflow was above the long-term average value, apparently freshwater was abundant during this period.

TABLE 9. HISTORIC AVERAGE INFLOW INTO THE GTC (2000-2015).

	Winter	Summer
Long-term average inflow m³/s	31.4	16.6
Obligated Two-month minimal inflow m³/s (Treaty value)	-	13

TABLE 10. SEASONAL AVERAGE INFLOW IN THE SCENARIOS.

Scenarios	B_1 & N_1		B_0 & N_0		B_2 & N_2	
	Winter	Summer	Winter	Summer	Winter	Summer
Lowest two month average inflow m³/s	-	8.6	-	12.8	-	18.7
Periodic average inflow m³/s	30.6	10.4	25.8	17.5	36.4	20.8

The realistic flow regimes have led to representative salt intrusion scenarios, imposing the same flow conditions allows us to make predictions about the magnitude of salt intrusion in the GTC after the implementation of the new lock.

6.2 Results of the Analysis

To allow a clear visualization of the tempo-spatial salinity variations, longitudinal salinity profiles of the GTC are illustrated in
Figure 6-2 up to Figure 6-19. With reference to the seasonal periods in Table 9 & Table 10, the salt profiles at approximately the end of winter (15th March) and after two months of low flow in summer (15th May) and at the end of summer (1th August) are visualized.
The salt profiles denote the concentrations and vertical gradients over the domain, up to 25 km upstream of the locks. A fixed colour scale is applied to make a transparent comparison between the baseline and the new set of scenarios. Besides evaluating general changes in the salinity dynamics, the criteria defined by the Dutch-Flemish treaty are reviewed to assess whether the current targets are still realistic after the reconstruction of the Terneuzen port. The international treaty states that circa 10 km upstream of the Terneuzen locks, at about 1 m below the free surface a maximum concentration of 5.8 ppt is allowed over two months. In the low flow period, the average inflow must not be lower as the target value of 13 m³/s, however the historic records already indicate that this target frequently is not met.

6.2.1 Low salt intrusion, scenarios B_2 & N_2

In the year 2008, the conditions in the GTC were highly favourable, the supplied amount of freshwater from Flanders was substantially higher than the long-term average, both in winter and in summer. The longitudinal winter salt profiles for the current locks (
Figure 6-2) and the new situation (Figure 6-3) show that locally near the locks the salinity concentration will be 0.5-1 ppt higher. Following the lock modification, the upstream concentrations are barely influenced and near Ghent the difference is negligible. The salinity in-out flux on the downstream boundaries is in balance, as salinity levels appear to be almost constant over winter.

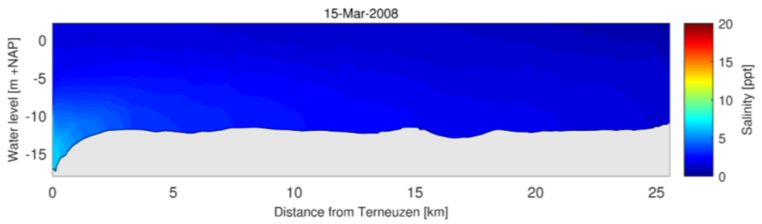

FIGURE 6-2. LONGTUDINAL PROFILE AT THE END OF WINTER, BASELINE SCENARIO B_2.

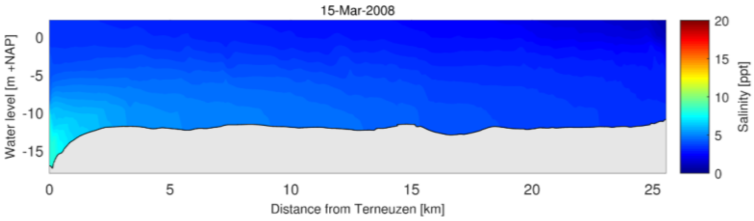

FIGURE 6-3. LONGTUDINAL PROFILE AT THE END OF WINTER, NEW SCENARIO N_2.

Two months into the summer, the salinity concentration appears almost the same as at the end of the winter period in the baseline scenario B_2 (Figure 6-4). The influx of salinity caused by the present lock is lower or equals the salinity flux. In the new scenario N_2 the salt intrusion in the direction of Ghent has started and salinity is gradually spread over the depth along the entire horizontal domain (Figure 6-5). The two month low inflow requirement of 13 m^3/s is not violated, and thus the magnitude of salt intrusion in the new scenario is limited.

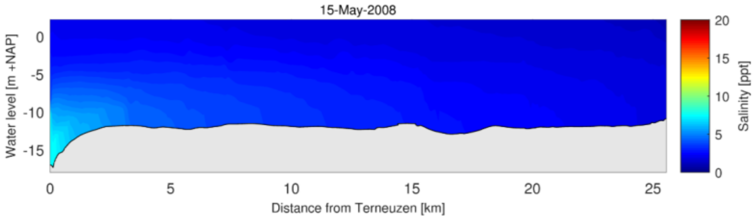

FIGURE 6-4. LONGTUDINAL PROFILE AFTER TWO LOW MONTHS IN SUMMER, BASELINE SCENARIO B_2.

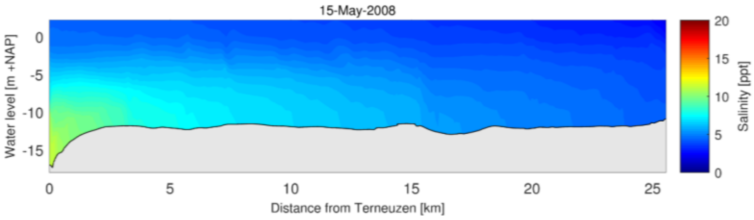

FIGURE 6-5. LONGTUDINAL PROFILE AFTER TWO LOW MONTHS IN SUMMER, NEW SCENARIO N_2.

Salinity concentrations progressively rise over the summer and after the low inflow months. At the end of summer the salinity concentrations in the baseline scenarios B_2 are highly favourable, approximately 10.5 km upstream the 5.8 ppt target is not even reached at the bottom (Figure 6-6) .

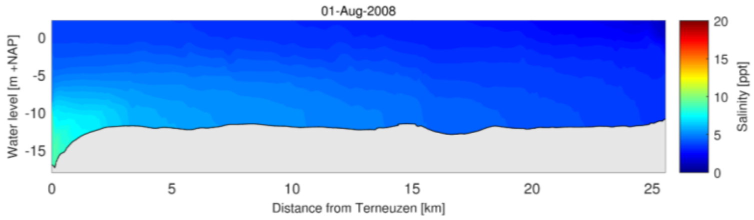

FIGURE 6-6. LONGTUDINAL PROFILE AT THE HIGHST SALINITY CONCENTRATIONS, BASELINE SCENARIO B_2.

As a result of the mitigating functions of the Terneuzen locks, the net salinity influx over the summer period is only small. Rather than observing a clear salt wedge, a moving salinity front can be seen in both situations. In Figure 6-7 it can be seen some stratification occurs near the locks after the modifications, but a few km upstream the concentrations are almost uniform over depth. At the end of summer, the differences in the two scenarios suggest that the concentrations are approximately twice as high near the lock and almost 2.3 higher near Ghent. Over the domain this increase shows a linear relation. Vertical salinity gradients remain marginal, the stratification rate increases with a maximum value 0.5 -1.5 ppt. In scenario N_2 as shown in Figure 6-7, the increased levels at the Dutch-Flemish border is exceeded. Further analysis reveals that the treaty value of 5.8 ppt is not exceeded over a 2 monthly period, but the discrepancy is smaller than 0.5 ppt.

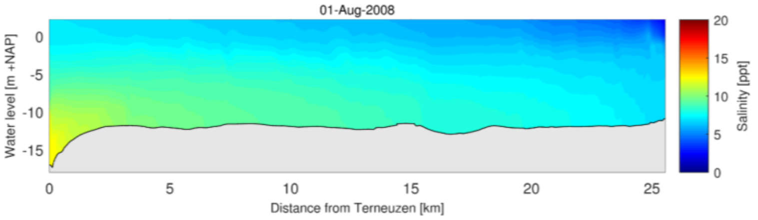

FIGURE 6-7. LONGTUDINAL PROFILE AT THE HIGHST SALINITY CONCENTRATIONS, NEW SCENARIO N_2.

After the construction of the new lock, the historic inflow conditions of a wet summer are barely sufficient to manage the salinity levels in the GTC.

6.2.2 Moderate salt intrusion, scenarios B_0 & N_0

In the moderate salt intrusion scenarios, the historical freshwater regime in the winter falls below the long-term observed averaged of 31.4 m^3/s, the average inflow was on only 25.8 m^3/s. Figure 6-8 shows that the freshwater amount appears sufficient in the baseline scenario B_0 to prevent salt intrusion into the GTC via the present locks. Saline density flows in the deeper layers transport salinity throughout the entire domain, at the end of winter the upstream concentrations are already slightly higher in the new scenario (Figure 6-9). In the baseline scenario B_0 it appears that salt intrusion affects the salinity levels up to approximately 5 km of the locks, further upstream background concentrations around 0.5 ppt are found. These background values are no longer visible in the new scenario, the saltwater influx from the new lock is too large to completely mitigate salt intrusion. Nonetheless, The salinity concentrations in the domain are constant over the winter in the new scenario N_0.

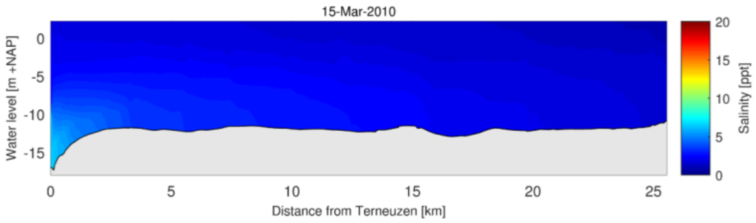

FIGURE 6-8. LONGTUDINAL PROFILE AT THE END OF WINTER, BASELINE SCENARIO B_0.

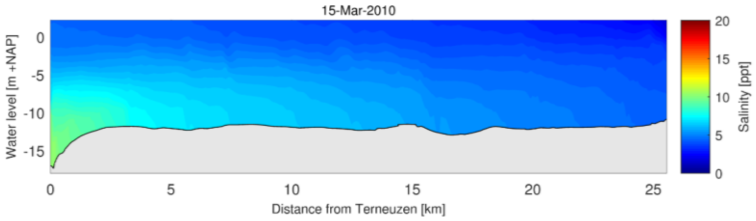

FIGURE 6-9. LONGTUDINAL PROFILE AT THE END OF WINTER, NEW SCENARIO N_0.

Because of the low winter inflow, the conditions at the beginning of summer were more brackish in comparison to the low salt intrusion scenarios. In the following two low inflow months, the salinity concentrations increase while the inflow reduces to almost the obligated average minimal of 13 m^3/s, the two month average inflow of 12.8 m^3/s is close to the treaty value. Figure 6-10 shows that in the baseline scenario B_0 the salinity concentrations are still low after the first 2 low flow months. The salt wedge remains in proximity of the locks. In scenario N_0 the salt wedge lies a lot further inland and saltwater intruded gradually in the upstream direction towards Ghent (Figure 6-11). After two low inflow months, the salinity target at 10.5 km of the locks is already exceeded in scenario N_0, and the concentrations keep on rising over summer.

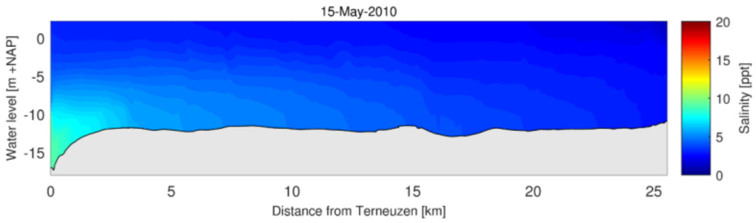

FIGURE 6-10. LONGTUDINAL PROFILE AFTER TWO LOW MONTHS IN SUMMER, BASELINE SCENARIO B_0.

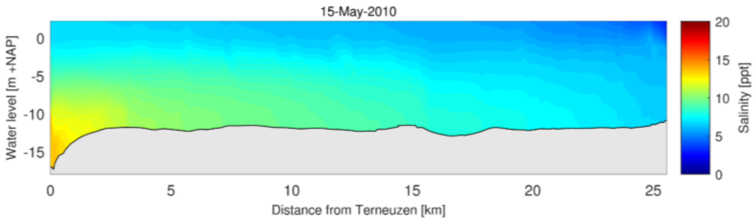

FIGURE 6-11. LONGTUDINAL PROFILE AFTER TWO LOW MONTHS IN SUMMER, NEW SCENARIO N_0.

Figure 6-12 and Figure 6-13 show the salt profiles at the end of summer for the baseline scenario B_0 and new scenario N_0. The average summer inflow was higher as the long-term average, therefore the baseline scenario B_0 resulted in an moderate salinization of the GTC. The salinity concentrations at the Dutch-Flemish border exceed the guideline of 5.8 ppt near the surface, but not on average over a two month period (Figure 6-12). In the new situation the treaty value appears no longer achievable, even with an near average summer inflow. The lack of water to flush back saltwater towards the Western Scheldt leads to an accumulation of saltwater in front of the locks and a clear salt wedge can be observed. Over the summer, the salinity concentrations far upstream in the domain become approximately two times higher and 1.8 times as high near the locks after the exchange flows are enlarged in the new scenario N_0. The salinization cycle simply occurs approximately twice as fast while the behaviour of salinity over the vertical plane remains similar. In the new scenario N_0 the vertical salinity gradient is approximately only 0.8-1.2 ppt higher at the end of summer in comparison to the baseline scenario B_0.

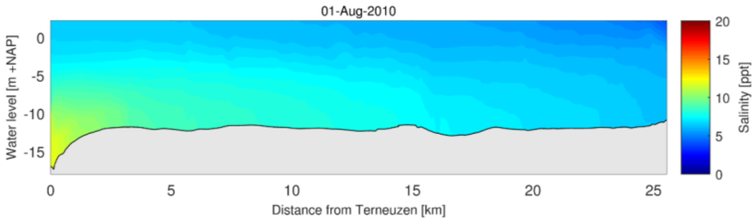

FIGURE 6-12. LONGTUDINAL PROFILE AT THE HIGHST SALINITY CONCENTRATIONS, NEW SCENARIO B_0.

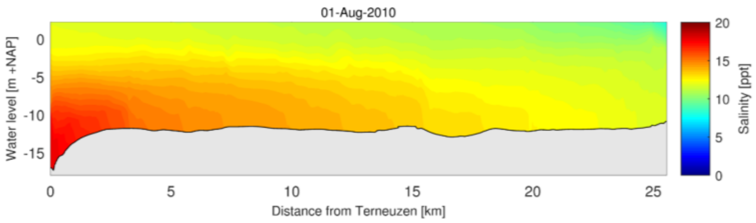

FIGURE 6-13. LONGTUDINAL PROFILE AT THE HIGHST SALINITY CONCENTRATIONS, NEW SCENARIO N_0.

6.2.3 Extreme salt Intrusion, scenarios B_1 & N_1

The historic inflow regime of 2011 resulted in extremely high salinity concentrations in the GTC. The baseline scenario B_1 shows the simulated concentrations at the end of winter (Figure 6-14). Over the winter months the inflow of 30.6 m^3/s was near the long-term average of 31.4 m^3/s. On the downstream boundaries the near average winter inflow is high enough to control the salinity in-out flux in the new scenario N_1, as salinity levels appear to be almost constant over winter. As can be seen in Figure 6-16 a new winter equilibrium situation will be established as the concentrations are approximately 1.8 near the locks and twice as high upstream when the salt profiles of the baseline scenario N_1 are compared. Similar as to the low and moderate salt intrusion scenarios N_0 and N_2 the impact of the lock modifications on the salinity concentrations is higher upstream, as the relative increase is the largest here.

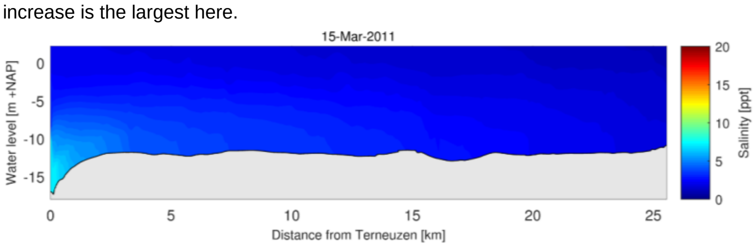

FIGURE 6-14. LONGTUDINAL PROFILE AT THE END OF WINTER, BASELINE SCENARIO B_1.

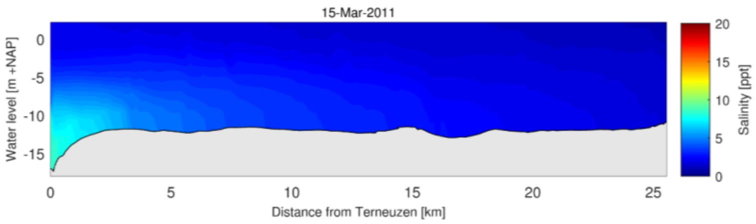

FIGURE 6-15. LONGTUDINAL PROFILE AT THE END OF WINTER, NEW SCENARIO N_1

After the winter period, the historic inflow in the extreme salt intrusion scenarios B_1 and N_1 drops far below the obligated minimal average of 13 m^3/s. As almost all available water is used for the levelling of the locks, the magnitude of the salt intrusion in the new scenario N_1 is the highest of all the simulated scenarios. Whereas Figure 6-16 shows that the salt intrusion in the baseline scenario B_1 has gradually led to higher salinity concentrations, in the new scenario N_1 a clear salt wedge has developed over the first two low inflow months (Figure 6-17). In summer, the high intrusion rate results in a fast increase of salinity concentrations over the domain and the maximum allowable salinity concentration of 5.8 ppt at the border is already exceeded after the first two summer months.

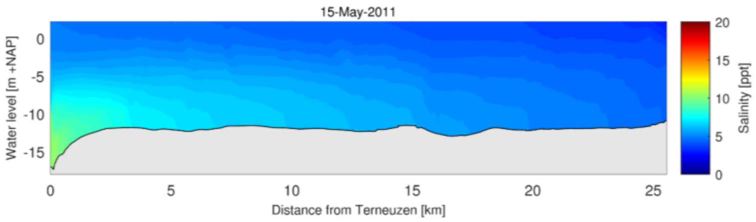

FIGURE 6-16. LONGTUDINAL PROFILE AFTER TWO LOW MONTHS IN SUMMER, BASELINE SCENARIO B_1.

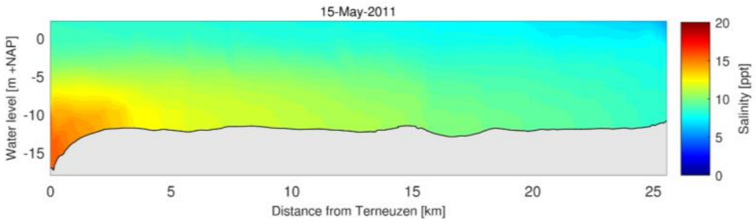

FIGURE 6-17. LONGTUDINAL PROFILE AFTER TWO LOW MONTHS IN SUMMER, NEW SCENARIO N_1.

The average summer inflow in the extreme salt intrusion scenario was below the long-term average value. The salinity concentrations at the end of summer for the baseline scenario B_1 and the new scenario B_1 are shown in Figure 6-18 and Figure 6-19 respectively. Both salt profiles show a full salinization in the GTC, the relative increase over summer is a factor 1.8 near the locks, this value linearly increases to a factor 2.0 for the upstream salinity concentrations, at the end of summer. In the new scenario N_1 the vertical salinity gradient is approximately only 1-1.5 ppt higher at the end of summer in comparison to the baseline scenario B_0.

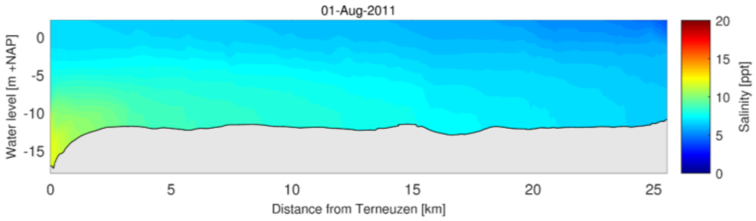

FIGURE 6-18. LONGTUDINAL PROFILE AT THE HIGHST SALINITY CONCENTRATIONS, BASELINE SCENARIO B_1.

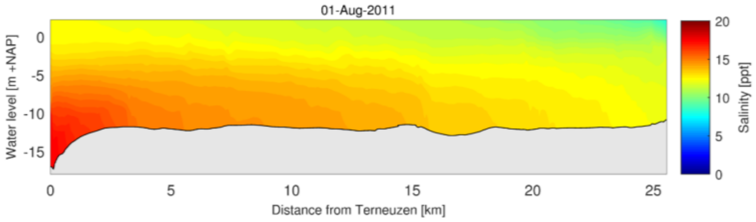

FIGURE 6-19. LONGTUDINAL PROFILE AT THE HIGHST SALINITY CONCENTRATIONS, NEW SCENARIO N_1.

In the extreme salt intrusion scenarios the salt profiles are shown at the end of summer, even though the actual low flow period lasted two months longer. The peak in the salinity concentrations is therefore even higher. Certainly, over the new scenarios the exchange flows will be proportionally larger and the transport of salinity via density flows occurs at a much faster rate. Primarily, as the duration of the low inflow period lengthens than it requires more decisive management to control the salinity concentrations in the GTC.

6.3 Conclusions

The results of the simulated salt intrusion scenarios showed the seasonal changes in the salinity dynamics of the GTC as a result of the planned lock modifications. From these results the subsequent conclusions can be drawn. In respect of the annual salinization cycle, the salinity concentrations in the GTC are estimated to be around twice as high upstream and 1.8 times higher near the locks, immediately after the modifications. The conclusions derived from the results of the Delft3D FM model agree with the findings of the EIA salinization study, who concluded that the salinity concentrations will increase by a factor of 2.5 following the construction of the new lock. However, the assessment in the EIA incorporated the influences of autonomous developments in the GTC in the salinity results. This factor was not examined in the scenario analysis with the Delft3D FM model, which explains why the EIA increase is relatively higher. In reflection upon the model error produced in the calibration procedure, the inaccuracy in the salinity results caused by uncertainties in the boundary conditions and inconsistencies in the verification data is only marginal in comparison to the deviations in the salinity levels caused by the lock modifications.

Evaluating the progressive increase of the salinity levels over summer confirms that the differences in salinity behaviour in the GTC are marginal, but the density driven salinity transport in the form of a salt wedge will become more significant, certainly in summer. When the bottom salinity starts to increase the rest of the water column rapidly follows. Therefore, under highly unfavourable summer inflow conditions, the stratification rate in the new scenarios will probably only become 1-1.5 ppt higher.

The relative increase of the salinity concentrations is larger upstream because saltwater intrudes further in winter. While a new winter equilibrium situations is established, the concentrations remain more or less constant over time, even in the scenarios B_0 and N_0 where the average inflow falls below the long-term observed average value. In general terms, the winter inflow appears sufficient to manage the salt intrusion in the GTC and the impact after the construction of the new lock is limited.

The historic flow regimes indicate that the minimal obligated freshwater supply of 13 m^3/s is not always reached, occasionally over a period of several months. During dry summers, the average inflow can even drop temporarily to 8.6 m^3/s over the first two low inflow months. The baseline scenarios demonstrate that the long-term average summer inflow is enough to meet the water quality requirements in the treaty. In the new scenarios, the average summer inflow appears to be too low to manage the salinity levels to conform with the treaty value, defined at the Dutch-Flemish border. The exchange rate of the new lock complex is so large that even under favourable summer inflow conditions the maximum allowable concentration is likely to be reached, thus complying with the current water quality standards appears no longer feasible in the near future.

Based on the present difficulties to allocate freshwater from Flanders towards the GTC, increasing the summer inflow seems no solution to the aggravated salinization problems. Mitigating measures to reduce the net saltwater influx, for example by limiting the maximum number of daily lock operations or installation of air curtains in the new lock, are more obvious solutions. However, due to the selecting of the particular new lock design, a more brackish state of the system is partially accepted by the Flemish-Dutch Scheldt committee and users must adapt their operations to more brackish conditions.

7 DISCUSSION

This chapter highlights the most important issues about the model setup, the overall modelling approach and the scenario analysis. The methods are compared to previous salinization studies in the GTC. Furthermore, we discuss how uncertainties are dealt with over the various modelling stages and these are denoted under three main headings. Last of all, the overall capability of Delft3D FM is reviewed and the applicability of the new hydrodynamic software is compared to the methodology used in the previous EIA salinization study.

7.1 Discussion about the Model Setup

For differing reasons, several factors were not accounted for in the model setup. For example, the influence of wind on the mixing processes near the free moving surface had not been incorporated in the model set up. In comparison to the mixing processes caused by the movement of vessels, the impact of wind was estimated to be proportionally lower and restricted to a few meters below the surface. Therefore, incorporating wind forcing in the GTC model would probably not increase the accuracy of the simulated surface salinity values. Another factor left out of the simulations were the water temperature variations. Water density is influenced by temperature gradients and the salinity concentration. Within the annual periodicity of salt intrusion in the GTC, small temperature variations in the water column occurred, however it was unlikely that noticeable temperature gradients over the horizontal plane would occur. There were no actual heat measurements performed to support this, thus it was assumed that local density was solely affected by the salinity concentration.

The schematization of various lock functions in the recently launched hydro software proved to be a challenging task, one from which now can be said that it was a far greater task than initially assumed. A considerable amount of knowledge, expertise and experience with 3D flow and salinity transport modelling was required to construct such a detailed and complex model of the GTC, capable of satisfying the general research objective. Adopting the modelling approach, similar to the setup of the 1D SOBEK model used in the salt intrusion studies in the EIA, was a logical step to follow. For some parts this turned out to be really promising as many of the boundaries conditions had been inventoried. However, simplifying the downstream boundary conditions into a single unit by combining the lock outflow and lock exchange of all locks, proved unsuccessful for the Delft3D FM model. The conditions on the downstream boundary quickly dominated the salinity behaviour over the entire domain, resulting in a quest for appropriate lock schematisation methods. The level of detail and complexity had to be raised, three individual boundaries with separate control structures were imposed, each connected by separated branches to the main channel. Relating to the SOBEK model, more data had to be acquired, processed and imposed by a means of coupled sinks and sources in the 3D model. This meant that the potential sources of uncertainties, inaccuracies and factors that had to be taken into account, tripled.

Imposing estimations of the lock exchange flows explicitly, rather than simulating the actual flow processes that cause the exchange of mass and momentum over the downstream boundaries, was a very effective and efficient way to reproduce the flow and salinity transport processes at Terneuzen. High numbers of hydrodynamic variables were clustered into a single parameter that could be scaled if necessary, although this method had some undesirable effects. With constant flows or pulses, the imposed exchange flows fitted the downstream boundaries, but a reduction to 21% of the estimated values became inevitable. In light of the available discharge data and the daily timescale of the freshwater inflow and the lock outflows, imposing constant flows appeared to be the best solution. Along with the historic flow data and the desire to establish a functioning GTC model, no alternative solutions were found to prevent scaling, even after distribution of the different locks induced flows over the vertical plane. It appeared that the salinity out-flux caused by the lock outflow was under-estimated and the GTC model was not fully able to reproduce the efficiency of flushing out saltwater via the lock culverts in the current Western and Middle locks, let alone what its real influence will be after lock modifications.

The steady flow distribution applied to the upstream discharge boundaries near Evergem and Moervaart did not conform to the observations, whilst the distribution varies over time. Imperfections caused by the firm distribution would undoubtedly have lead to small deviations in the salinity profile between the mouth of the Moervaart and the inflow at Evergem. A variable flow distribution over the seasons, in which there will be more inflow through the sluice at Evergem, will have direct consequences as salinity concentrations upstream strongly respond to changes in the discharge. Probably the lateral salinity profiles will show an even steeper gradient across the depth because the influence of the freshwater inflow is the largest near Ghent. At the Flemish-Dutch border, both upstream boundaries discharged freshwater in the channel, so for the Dutch domain of the GTC the influence of an imperfect discharge distribution from Ghent no longer played a role and the uncertainty caused by this factor diminished.

7.2 Discussion about the Calibration Procedure

The basics of salinity modelling start with the reproduction of all flow processes that control the transport of scalar quantities like salinity. To verify the 3D models ability to reproduce the hydrodynamic conditions in the GTC, historic records of salinity and flow variables were required, yet the data availability was restricted to a limited amount. First of all, flow velocity measurements have never been recorded, velocity data records would have been useful to support the presence and importance of density driven flows in the GTC. In particular the absence of high frequent bottom salinity data brought some uncertainty to the model results. Periodic depth measurements were used to gain an indication of the stratification degree over four observation points in the GTC, but this data only contained six measurements per year, a number too restricted to make solid statements about the behaviour of the bottom salinity and density driven salinity transport. Moreover, these measurements were collected by boat, suggesting that these records may contain small errors caused by spatial differences. Obviously, some accuracy was lost in translating the salinity values into the part per thousand values used by Delft3DFM, though in the light of the statistical errors produced in the calibration, the impact was minimal.

The calibration process resulted in an extensive search for the optimal parameter setting, while scaling of the exchange flows resulted in an additional calibration factor. Changing boundary conditions during the calibration procedure was somewhat controversial, and brought ambiguity to the models ability to simulate futuristic scenarios. The Delft3D FM model reproduced the historic salinity dynamics on a detailed scale and all physical flow and transport processes were embedded in the model, though it remained questionable whether scaling always lead to representative conditions on the downstream boundaries after lock modifications. In the less detailed 1D models, this uncertainty factor could be estimated with minimal efforts, by assessing how sensitive the salinity levels were when a variety of scales were used for the exchange. Performing a comprehensive sensitivity analysis for the Delft3D model was optional, but went beyond the objective and timeframe of this thesis. The predictive power of the Deflt3D FM GTC model has not been proven beyond doubt, but one can presume that the hydrodynamics in the simulation of futuristic scenarios are more accurate than in the 1D SOBEK model of the GTC, especially given the high values for R^2 in the reproduction of historic salinity levels. Besides, the trend in the few bottom salinity measurements show similarities with the simulated salinity values.

An important aspect in the calibration procedure was the use of different salinity records. In the modelling study of the EIA, the calibration was performed depth averaged. The average value, composed from the average of two salinity records were both measured in the top half of the longitudinal wet profile. Simulations with Delft3D FM suggest that this was a conservative estimate of the salinity in the GTC, while the actual salinity levels at the bottom were higher. Therefore, the depth average values were slightly underestimated. It explained why a successful calibration of the GTC 3D model could only be obtained with depth variable salinity measurements at the surface and bottom. Although, the salinity concentrations produced in the calibration by the 3D model were overall higher, the predictions of present and future scenarios are likely to be more realistic.

7.3 Discussion about the Scenarios

The focus in the scenario analysis directed to instant changes in the GTC salinity dynamics due to lock modifications. The exchange flow at the Middle lock had been increased to examine the impact of lock modifications under seasonal variety of fresh water inflows. In reality there will be more to it, construction of the new lock would change the design of the inner port, the flow patterns near the locks would change and a separate sluice would be installed to control the water level in the GTC. These local changes were not integrated in the GTC model, while their influences were likely restricted to a few km upstream of the locks. Vessels of the largest category gain access to the GTC in the near future but to allow save passing of ships, the channel might need to be dredged.

In the scenario analysis, the impact of climate change and economic developments had not been examined. Although these factors were not part of the research objective, the possible impact of these factors are worthwhile mentioning. Autonomous developments of the GTC, will lead to an intensification of traffic in the waterway, inherently the number of lock operations will increase. The lock exchange ratios will not necessarily become larger, but the values of the exchange flows will certainly rise, especially for the new lock a single operation greatly contributes to the total daily exchanged fresh-saline water volume.

Climate change influences the salinity dynamics in the GTC in multiple ways, rising sea levels mean higher water levels in the outer port of the Terneuzen lock. Climate studies indicate a maximum rise of 35 cm in the water level of the Western Scheldt by the year 2050 (Deltares, 2013). Gradually over the tidal cycle, water levels will increase, the pressure differences will becomes smaller and there will be less time to discharge saline water back into the outer ports. Moreover, the influx of saltwater will be larger, whereas the percentage of water from the Western Scheldt in the lock chamber will be higher. Obviously, the lock exchange ratios are affected by this, the higher the salinity content in the locks will be, the faster and stronger the density flows will be after opening of the lock door on the GTC side.

Climate change is a slow process and the exact time scale and magnitude on the freshwater inflow is unknown. The most recent climate models assume that the base inflow (- 35%) and two month average low flows (- 45%) from Flanders are likely to decrease in summer. In the winter, the average inflow is estimated to be higher (+ 2%) by 2050 (Deltares, 2013). The intensity of peak flows would however increase (Vanderkimpen et al., 2012 ; Lebbe, 2009). The possible event of a decrease in base flow in summer, would mean that the intensity increase of peak flows is welcome, this would make it possible to replenish the stored water volume and to set up more frequent flush regimes.

7.4 Delft3D FM Application Review

Looking back at using the Delft3D FM application to investigate the impact on salinity dynamics in the GTC following the planned new lock modifications, the new hydro software proved to be more than capable of simulating salinity levels on a detailed scale. By simulating the vertical salinity gradients and the salt wedge migration, the model gave some renewed insights about the vertical salinity distribution in the domain that cannot be estimated with conventional 1D models. In comparison to the predecessor of Flexible Mesh, the use of un-structured grids were a welcome addition, because they offered the needed flexibility to connect the various ports and branches towards the locks. Also, due to the new algorithms and discretization methods the simulation time was probably significantly reduced, in the highly resolved computations this lowers the runtime. However, it was really unfortunate that the post-processing output tools for Delft3D FM were not fully operational as yet, this made it much harder to get those first important impressions and to visualize the results.

Finally, running multiple scenarios with the current GTC Delft3D FM model is still quite ambiguous whilst it is time-consuming to create new time series for the various control structures. Temporal changes in the storage capacity of the GTC cannot be addressed. The encountered issues are the result of a strict water balance in the model. Seeking for alternative methods to autonomously let the model control the water balance rather than using discharge time series, might not only eliminate the use of a low-fixed time step, it will make the models better editable and more user friendly.

8 CONCLUSIONS & RECCOMENDATIONS

The research methodology and the subsequent findings have already been discussed in preceding chapters. In this final chapter the conclusions are enumerated per research question and it assesses in how far the overall research objective has been achieved. Finally, recommendations are made for possible follow-up studies and areas for improvements in 3D salinity modelling in Delft3D FM are evaluated.

RQ 1. How can we setup a 3D Delft3D-FM model of the GTC?

The model setup of the SOBEK 1D model, used in the EIA study, has contributed greatly in the setup of the Delft3D FM model. An important conclusion is that in such complex 3D schematisations the flow and salinity transport processes at the locks, the same methodology is no longer appropriate. The explicit method, where the results of detailed simulations were used to estimate the fresh-saline lock exchange, was however successfully adopted from the EIA. It demonstrates that using these explicit methods of imposing exchange flows is a very time efficient and effective way to implement incoming salt fluxes through lock operations. In order to reproduce the flow patterns and salt transport processes accurately near the connections of the various ports, flexible connections were used. The predecessor of Delft3D only allows curvilinear grid adjustments, and this is therefore an important and welcome improvement. In complement, the new discretization methods in Deflt3D FM enables significantly faster computations, a point that becomes more important when large computational capacity is required, like for the GTC 3D model.

RQ 2. How well can this model reproduce salinity levels in the GTC?

The lack of hydrodynamic variables like discharge or flow velocity records meant that the calibration and validation procedure could only be performed with salinity measurements in the GTC. The ability of the Delft3D FM model to reproduce the tempo-spatial salinity changes, was successful examined with the aid of the statistical indicators RMSE and the R^2. With the optimized parameter set, the Delft3D FM GTC model reproduced satisfactory salinity results under various inflow conditions the domain. Especially upstream, the salinity levels near the bottom and at the free surface were reproduced more accurately under highly brackish conditions in the calibration period. This is an important conclusion as predications were made with the Delft3D FM model of the GTC under even more saline conditions, whilst the salinization is likely to increase by the planned lock modifications. It does not necessarily mean that the model cant reproduce representative salinity concentrations in years with low salt intrusion. High R^2 value around 0.9 for the stations located more than 3.5 km away from the locks denotes the strong linear association between the observed and simulated values over the calibration and validation period. Given the variety of salinity over the calibration and validation periods, the largest errors may be considered too high, but in general the (RMSE) and the relative (NRMSE) are not uncommon and probably in the same range of the errors produced in the study of the EIA.

Given the large amount of assumptions that were needed to be made to impose good conditions on the downstream model boundaries and the uncertainty in the flow and bottom salinity data, it was considered to be a proper result, comparable in quality to the results of the SOBEK 1D model used in de EIA. However, the physics are better embedded in the Delft3D FM model. With respect to the planned lock modifications, this raised that level of confidence in simulating future scenarios.

RQ 3. How are the salinity dynamics in the GTC affected by the planned lock modifications?
The impacts of the lock modifications were investigated by running scenarios with the current lock exchange flow and for the new situation with historical inflow series that led to three representative salinization scenarios, respectively low, moderate and an extreme salt intrusion into the GTC. Over the winter, the salinity concentrations will remain constant although the values will approximately be twice as high after immediate lock modifications. Obviously, because of the planned lock modifications the salt wedge will influences the concentrations over the full length of the GTC, but the effect is limited in the winter. In the summer, the consequences of the lock modifications are larger, over this period the salinity concentrations will probably increase at least 1.8- 2 times faster, however the duration of the low flow period determines the maximum salinization of the GTC. Therefore it can be concluded that the water quality standard, defined in the treaty is no longer feasible in the near future. The variety of salinity of the vertical plane undouble increase, but the trend of the annual salinization of the GTC will probably not change. In summer, as the salt wedge draws inland then the gradual salinization of the entire water column follows quickly. Meaning that in high salt intrusion scenarios, the stratification rate will probably only be 1-1.5 ppt higher. The application of a 3D model was essential to arrive at these conclusions. In addition, because of the future increase in the salt intrusion, mitigation measures in the new lock might be the best solution, but inherently the local users must adapt to a more brackish state of the GTC.

The aim of this thesis was to predict salinity dynamics in the GTC due to the planned lock modifications with a Delft3D FM model. From a broader perspective, we can conclude that the new hydro software is well capable of simulation these changes on an accurate and detailed scale. For this specific case 3D modelling gave clearer insights in the density driven salinity transport in the GTC. However, the general Delft3D FM model conclusions overall agree with the results of the conventional 1D model in the EIA.

8.1 Recommendations

It is recommended to carry out additional measurements over the longitudinal profile of the GTC. High frequent flow velocities and discharges and bottom salinity concentrations are currently not monitored in the GTC, comparing observations of the water movement and bottom salinity data will help lower model uncertainties. Furthermore, wind speed data is currently available and can be introduced into the model to make a more accurate prediction using the Delft3D FM model. The new model Delft3D FM is undergoing constant developments, features that are currently only available for Delft3D will in the short-term also provide solutions for the inconveniences that currently exist in the Delft3D FM salinity transport model of the GTC. The universal basis of the new generate hydro model offers a variety of possibilities. Flow and salinity processes can already be simulated in detail, but with developments in the Delft3D FM model, the GTC model will also be suitable for investigating thermodynamic processes or investigating the spread of pollutants. Furthermore, instead of using implicit methods to simulate lock exchanges, a full scale model capable of predicting the real fresh-saline lock exchange becomes a realistic possibility.

In future follow-up studies, more attention needs to be given to the scenario analysis. Given that time and resources were restricted, this investigation has been limited to some representative scenarios. However, a broader assessment of future effects is recommended. The impacts of climate change on the inflow of Ghent and the impacts on the water levels and salinity concentration in the Western Scheldt were not addressed herein. Also, economic developments in the GTC will lead to more navigational activity, it is highly likely that increasing the number of lock operations will have a greater impact on the magnitude of saltwater intrusion over time. Finally, an important findings is that the application of the 3D control structures in Delft3D FM can be optimized. It is recommended that the real-time control feature, currently already available in the 1D module in the Delta shell, will be made available for all 3D modelling purposes in Delft3D FM. This feature allows the autonomous control of the water balance in the model. Running flow scenarios would then require less effort, it might solve the fixed-low user time step in the GTC 3D model and simultaneously accounts for some storage capacity over the domain.

BIBLIOGRAPHY

Arcadis. (2007). *Technische en kosten studie met nautische toets. Fase 4.* retrieved from http://nieuwesluisterneuzen.eu/

Augustijn, D., van den Berg ·, M., & Korving, H. (2011). *Dynamic Control of Salt Intrusion in the Mark-Vliet.* Water Resources Management. doi:10.1007/s11269-010-9738-1

Bombardelli, F., Cantero, M., Garcia, M., & Buscaglia, G. (2010). Numerical aspects of the simulation of discontinuous saline underflows: the lock-exchange problem. *Journal of Hydraulic Research, 47*(6), 777–789. doi:10.3826/jhr.2009.3238

Breemen, M. (2008). *Salt intrusion in the Sengelor Esturary Malaysia.*

Callens, M., & Keps-Heyndrickx, Y. (1983, March-April 9). Bestrijding van de verzilting van het kanaal Gent-Ternzeuzen. *Water N'*.

Deltares. (2012). *KPP Verziltingsbestrijding: Inventarisatie schutsluizen RWS m.b.t zoutindringing. Begeleidende factscheets.*

Deltares. (2013). *Deltascenario's 2012 NHI modelinvoer : Technische achtergrondrapportage.* www.helpdeskwater.nl

Deltares. (2015). *Delft3D Flow User manual.*

Deltares. (2016). *D-Flow User manual.*

Deltares. (2016). *Quickplot User Manual.*

Donchyts, G., Baart, F., Van Dam, A., & De Goede, E. (2014). Next generation hydro software.

FDSC. (2015). *Millieu Effecten Rapportage.* retrieved from http://nieuwesluisterneuzen.eu

Gross, E., Koseff, J., & Monismith, S. (1999). Three-Dimensional Salinity Simulations of South San Fransico Bay. *Journal of Hydraulic Engineering*.

Kerstma, , J., Kolkman, P., Regeling, H., & Venis. (1994). *Water Quality control at ship locks. Prevention of salt and fresh water exchange. A.A. Balkema, Rotterdam/Brookfield.*

Lamboo, M. (2014). *Capaciteitsanalyse van de Prinses Margrietsluis in Lemmer Master Thesis.* Civiele Techniek en Geowetenschappen. TU Delft. retrieved from http://repository.tudelft.nl/

Lebbe, L. (2009). *Haalbaarheids onderzoek Seine-Schelde West: Verkennend onderzoek over de waterbeschikbaarheid en verziltingaspecten.* Universiteit Gent.

Lyman, J. (1969). Redefinition of salinity and chlorinity. *Limnology and Oceanography, 14*, 928-929.

Nguyen, A. D. (2008). *Salt Intrusion, Tides and Mixing in Multi-Channel Estuaries.* doi:10.1201/9781439828342

Santosa, S., v.d. Wegen, M., Reyns, J., v. Dam, A., Solomatine, D. P., & Roelvink, J. (2014). Multi station calibration of 3D flexible mesh model: Case study of the Colombia Estuary. *Elsevier*.

Shaha, D. C., & Cho, Y. (2009). Comparison of empirical models with intensively observed data for. *Hydrolic earth system sciences, 13*, 923–933.

Steenkamp, B. (2004). *Systeem en proces beschrijving Noordzeekanaal Een kennisInventarisatie.* RIZA.

Svašek. (2010). *Invloed nieuwe voorkeursvariant op chloride concentratie in het kanaal Gent-Terneuzen.*

Svašek. (2012). *Verkenning maritieme toegankelijkheid: Aanvullend oppervlaktewater onderzoek.*

UNESCO. (1996). *The final resolution of the symposium on the classification of brackish waters.*

Van Damme, S., Struyf, E., & Maris, T. (2005). Spatial and temporal patterns of water quality along the estuarine salinity gradient of the Scheldt estuary. (E. M. Department of Biology, Red.) doi:10.1007/s10750-004-7102-2

van Drakestein, F. (2014). *Modeling of tides and spreading of saline water in the Arabian Gulf and in the coastal area of Abu Dhabi with a flexible mesh model.*

Vanderkimpen, P., Pereira, F., & Mostaert, F. (2012). *Deelrapport 7 - Zoutintrusie kanaal Gent-Terneuzen.* Waterloopkundig laboratorium.

Waterloopkundiglaboratorium Delft. (1988). *Zoutbestrijding volgens het systeeem terneuzen.* Rijkswaterstaat.

APPENDIX I. LOCK CYCLES

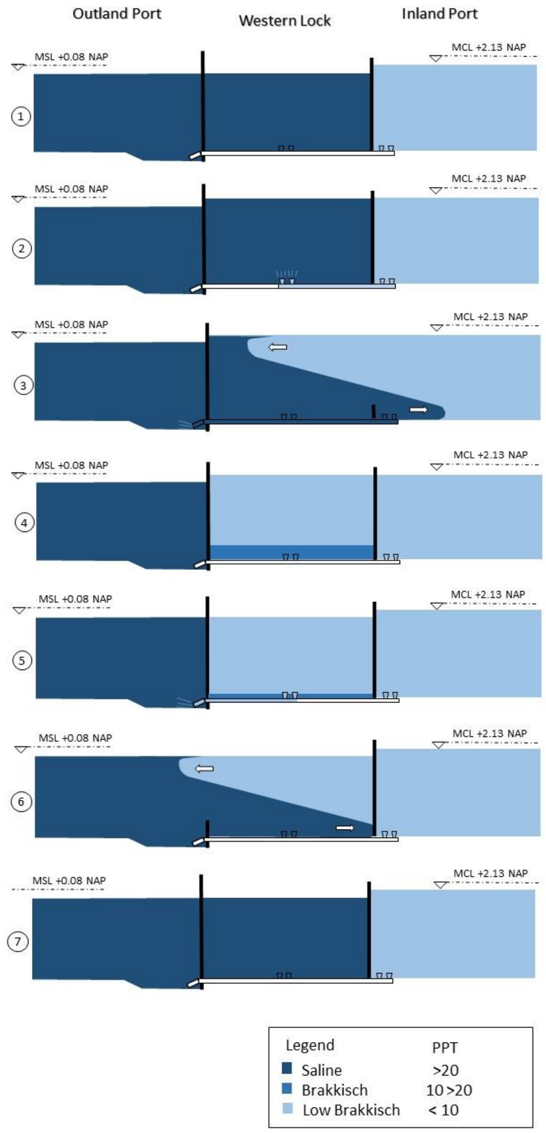

1). The outer lock doors is open and ships enter the lock chamber from the Western Scheldt.

2). The outer lock doors closes and the water level in the lock chamber is levelled towards the GTC level, by employing the locks culverts. Channel water is used for levelling.

3). The inner lock doors open and ships navigate towards the GTC. Immediately after opening of the doors the density flows emerge and fresh channel water and saline water in the lock chamber is exchanged.

4). A mixed brackish layer remains between the lock sills. Ships navigating towards the Western Scheldt enter the lock. The inner lock doors close.

5). The lock chamber is levelled towards the level in the Western Scheldt .

6). The outer locks door open and ships navigate towards the Western Scheldt. Similar to step 3, density flows emerge and the lock content will (partially) be exchanged.

7). A full lock cycle is completed, the conditions in the lock chamber are equal to step 1 are the density flows vanish over time.

APPENDIX II. ESTIMATION OF THE LOCK EXCHANGE

The results of the initial simulations with the FINEL3D model to estimate the exchange ratios of the lock chambers are shown in Figure 0-1 up to Figure 0-4, based on the average tidal level in the Western Scheldt.

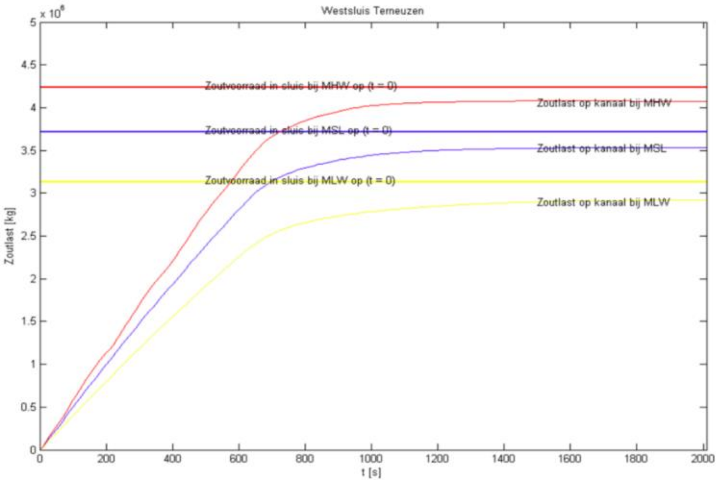

FIGURE 0-1. EXCHANGE OF THE INITIAL SALTLOAD OVER TIME AT THE WESTERN LOCK FIGURE TAKEN FROM (SVAŠEK, 2010)

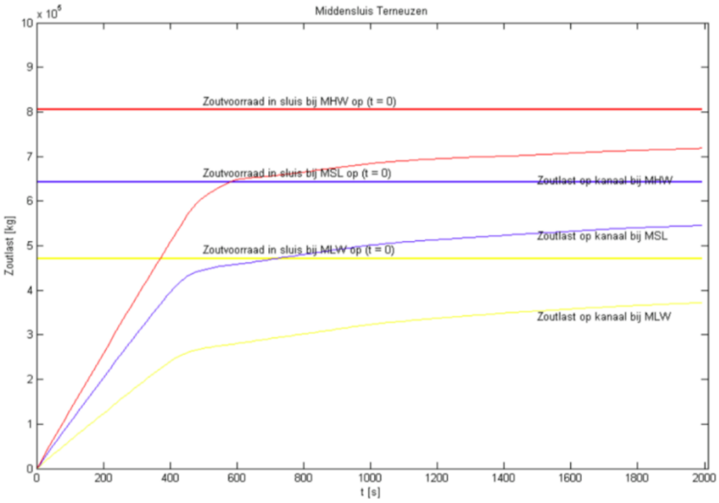

FIGURE 0-2. EXCHANGE OF THE INITIAL SALTLOAD OVER TIME AT THE MIDDLELOCK FIGURE TAKEN FROM (SVAŠEK, 2010)

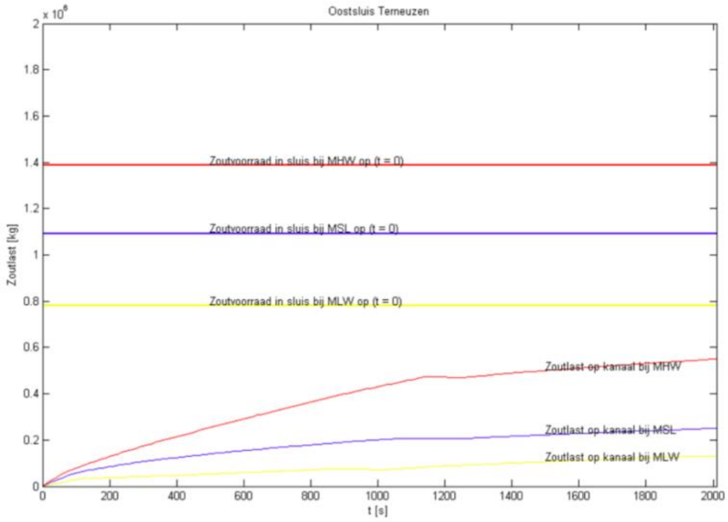

FIGURE 0-3. EXCHANGE OF THE INITIAL SALTLOAD OVER TIME AT THE EASTERN LOCK (SVAŠEK, 2010)

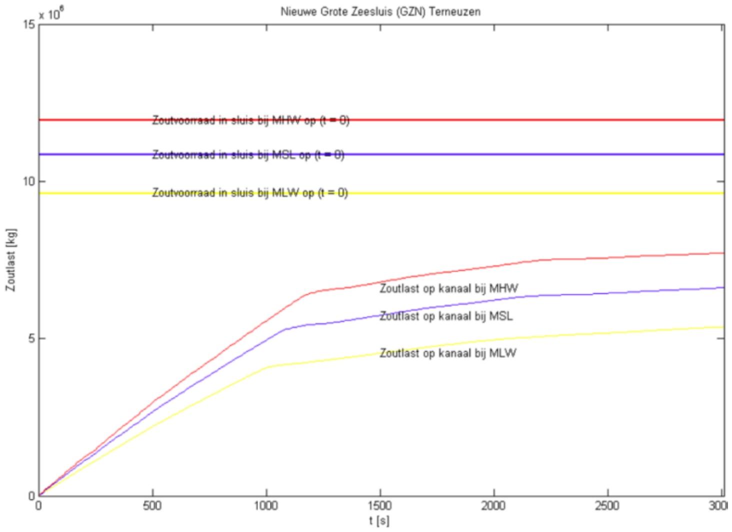

FIGURE 0-4. EXCHANGE OF THE INITIAL SALTLOAD OVER TIME AT THE NEW LOCK FIGRUE TAKEN FROM (SVAŠEK, 2010)

Commented [JvdW2]: Leg je deze figuren ergens uit?

APPENDIX III. LONGTUDINAL SALT PROFILES

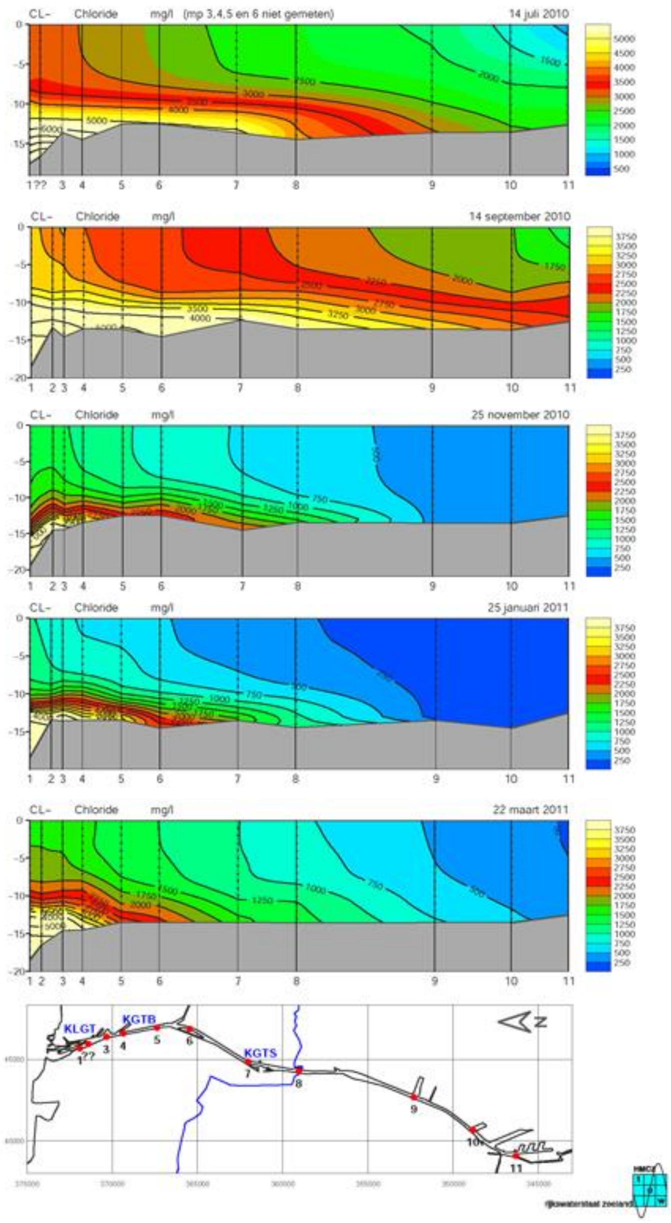

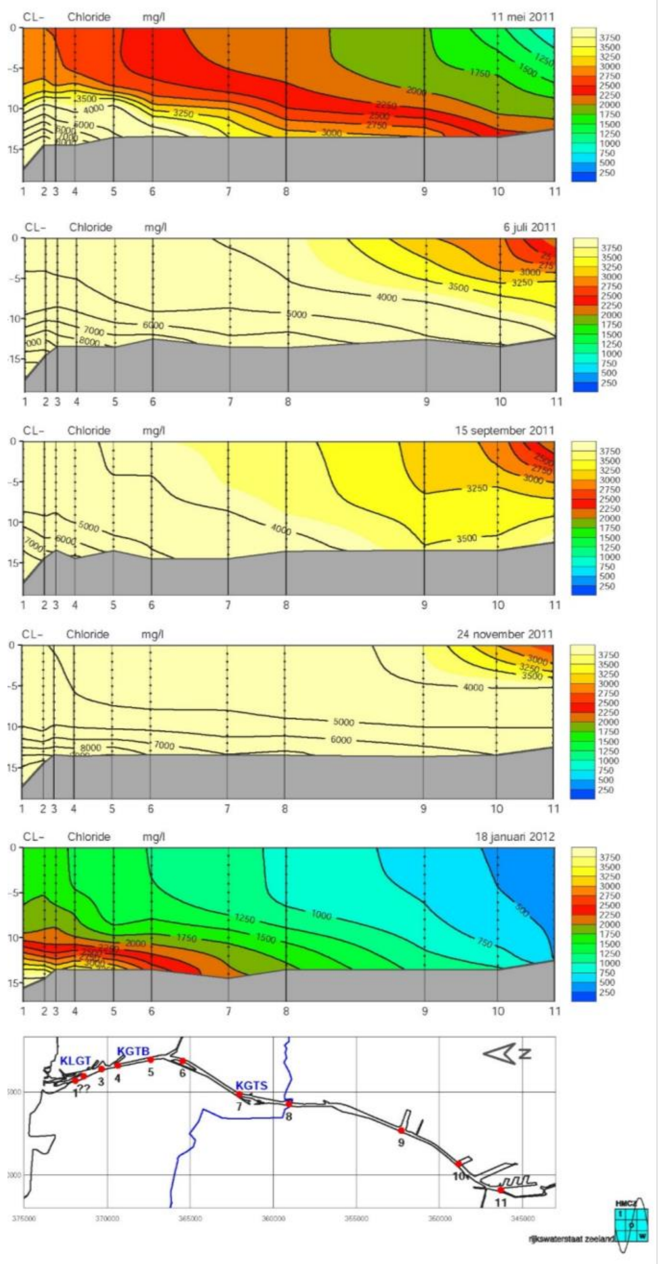
CL- Chloride mg/l
11 mei 2011
6 juli 2011
15 september 2011
24 november 2011
18 januari 2012
KLGT
KGTB
KGTS
rijkswaterstaat zeeland

APPENDIX IV. SENSITIVITY ANALYSIS

The results of all simulations performed in the sensitivity analysis of Section 5.2 are shown below.

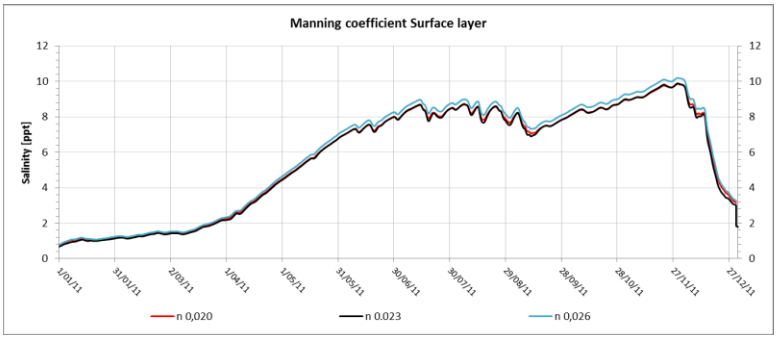

FIGURE 0-1. VARIATION OF SURFACE SALINITY FOR THE BOTTOM ROUGHNESS, 10.5 KM UPSTREAM OF THE LOCKS.

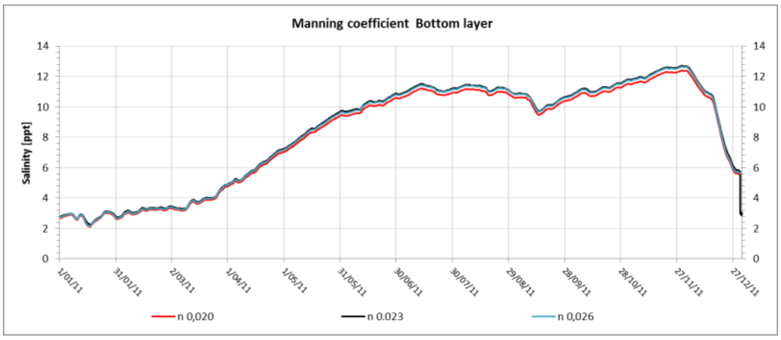

FIGURE 0-2. VARIATION OF BOTTOM SALINITY FOR THE BOTTOM ROUGHNESS, 10.5 KM UPSTREAM OF THE LOCKS.

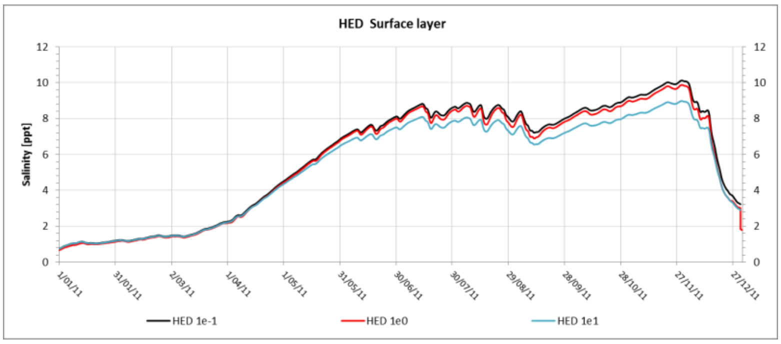

FIGURE 0-3. VARIATION OF SURFACE SALINITY FOR HED, 10.5 KM UPSTREAM OF THE LOCKS.

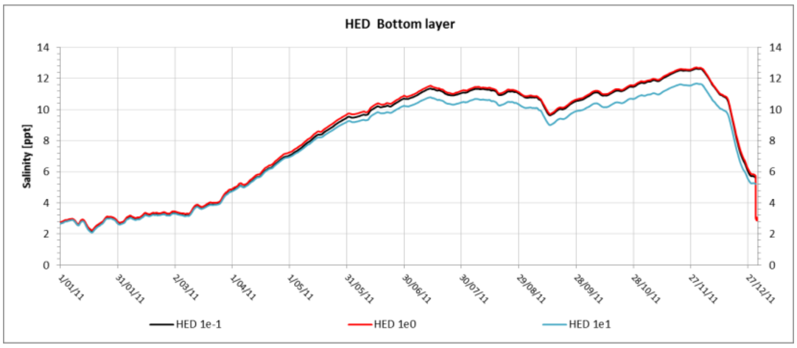

FIGURE 0-4. VARIATION OF BOTTOM SALINITY FOR HED, 10.5 KM UPSTREAM OF THE LOCKS.

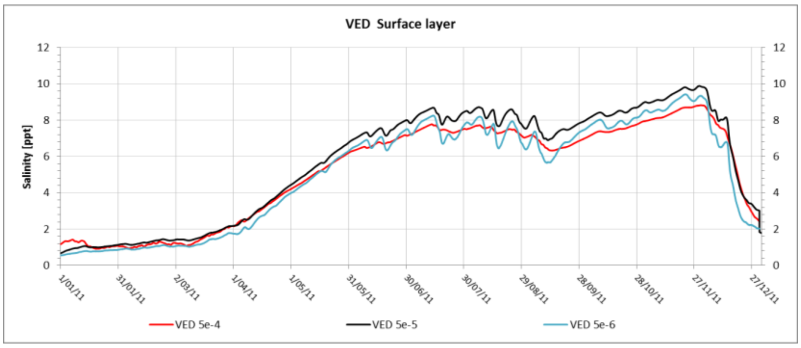

FIGURE 0-5. VARIATION OF SURFACE SALINITY FOR VED, 10.5 KM UPSTREAM OF THE LOCKS.

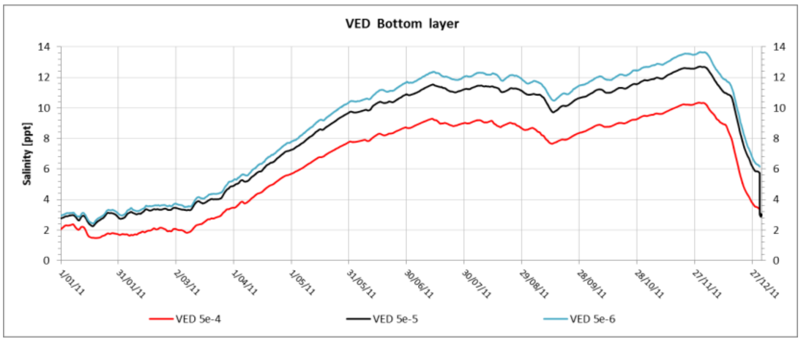

FIGURE 0-6. VARIATION OF BOTTOM SALINITY FOR VED, 10.5 KM UPSTREAM OF THE LOCKS.